International Journal of Hydrogen Energy 143 (2025) 846–861

Contents lists available at ScienceDirect

International Journal of Hydrogen Energy

journal homepage: www.elsevier.com/locate/he

Energy, exergy, exergoenvironmental, and exergoenviroeconomic assessment of a two stroke UAV small engine using JP5 aviation fuel and hydroxy (HHO) gas

S. Özer [a], E. Tunçer [b,c], U. Demir [d], H.E. Gülcan [e], S. Çelebi [f,g,*]

[a] Department of Mechanical Engineering, Muş Alparslan University, Muş, Turkey
[b] Erin Engine Corporation Inc., Department of Research and Development, İstanbul, Turkey
[c] Department of Mechanical Engineering, Faculty of Engineering and Natural Sciences, İstanbul Health and Technology University, İstanbul, Turkey
[d] Department of Mechanical Engineering, Bilecik Şeyh Edebali University, Bilecik, Turkey
[e] Department of Mechanical Engineering, Faculty of Technology, Selçuk University, Konya, Turkey
[f] Motor Vehicles and Transportation Technologies Dep., Arifiye Vocational School, Sakarya University of Applied Science, Sakarya, Turkey
[g] Automotive Technologies Application and Research Center, Sakarya University of Applied Sciences, Sakarya, Turkey

ARTICLE INFO

Handling Editor: Ramazan Solmaz

Keywords:
Energy
Exergy
Environmental and economic analysis
UAV smallengine performance
Emissions

ABSTRACT

Hydroxy gas (HHO) is a gas produced by the electrolysis of water, which involves breaking down water molecules (H_2O) into hydrogen (H_2) and oxygen (O_2) gases. When the electricity used for electrolysis comes from renewable energy sources, the resulting hydrogen can be classified as 'green hydrogen.' Therefore, by using renewable green energy sources to produce HHO gas, its application in internal combustion engines can promote clean combustion and enhance sustainability. This study explores the enhancement of performance and emission characteristics in a two-stroke Unmanned Aerial Vehicle (UAV) engine using Hydroxy gas (HHO), a green energy source produced via water electrolysis. The primary objective is to improve engine efficiency and reduce environmental impacts by employing HHO in dual-fuel mode with JP5 aviation fuel. Addressing a clear research gap in the literature, this study is the first to evaluate the energy, exergy, exergoenvironmental, and exergoeconomic aspects of a two-stroke, air-cooled UAV engine using the JP5+HHO fuel blend. Experiments were conducted at five shaft speeds (3250, 3750, 4500, 5250, 6250 rpm) and four HHO flow rates (1.0, 1.5, 2.0, 4.0 lpm). The results demonstrate that incorporating HHO gas leads to a significant improvement in engine performance, with a 10% average reduction in Brake Specific Fuel Consumption (BSFC) and a 10% increase in exergy efficiency. Additionally, the JP5+HHO 4 lpm mixture reduces exergy destruction by approximately 10% and increases heat transfer exergy by 3–10%. On the environmental front, while HHO slightly increases CO_2 emissions, the exergoenvironmental impact rises by a manageable 4%. Importantly, the high HHO flow rate (4 lpm) achieves a 2% average reduction in both exergoenvironmental and exergoeconomic impacts. These findings underscore the potential of HHO as a sustainable fuel source, offering both performance gains and reduced environmental and economic costs.

1. Introduction

Unmanned Aerial Vehicles (UAVs) have become increasingly important in various sectors, including military, commercial and scientific research, due to their versatility and efficiency [1,2]. UAVs are used in military operations, construction, package delivery, mapping, medical services, search and rescue missions, exploration of hidden areas, monitoring of power lines and oil rigs, precision farming, aerial surveillance, and wireless communications [3,4]. In the medical field, UAVs are used for vaccines, automated external defibrillators, and hematological products, as well as for public health surveillance [5]. The breadth and capabilities of UAVs, their performance and durability are highly dependent on the capabilities of their propulsion systems, primarily internal combustion engines [6,7]. two-stroke spark ignition engines are widely used in UAVs due to their high power-to-weight ratio, simplicity and cost effectiveness [8,9]. However, these engines face significant challenges regarding fuel efficiency and exhaust emissions,

* Corresponding author. Motor Vehicles and Transportation Technologies Dep., Arifiye Vocational School, Sakarya University of Applied Science, Sakarya, Turkey.
E-mail address: scelebi@subu.edu.tr (S. Çelebi).

https://doi.org/10.1016/j.ijhydene.2024.10.394
Received 6 September 2024; Received in revised form 24 October 2024; Accepted 28 October 2024
Available online 12 November 2024

Nomenclature

UAV	Unmanned Aerial Vehicle
HHO	Hydroxy Gas (Oxyhydrogen)
JP5	Jet Propellant 5 (Aviation Fuel)
BSFC	Brake Specific Fuel Consumption
BTE	Brake Thermal Efficiency
EGT	Exhaust Gas Temperature
EST	Engine Surface Temperature
CO	Carbon Monoxide
CO_2	Carbon Dioxide
HC	Hydrocarbons
NO_x	Nitrogen Oxides
O_2	Oxygen
η	Efficiency
$\dot{m}$	Mass Flow Rate (kg/s)
Q	Heat Transfer Rate (kW)
W	Work Output (kW)
X_e	Exergy Flow (kW)
I	Irreversibility (kW)
rpm	Revolutions Per Minute
kW	Kilowatt
MJ	Megajoule
LPM	Liters Per Minute
T	Temperature (K)
T_o	Reference Temperature (K)
h	Specific Enthalpy (kJ/kg)
s	Specific Entropy (kJ/kg·K)
P	Pressure (Pa)
R	Specific Gas Constant (kJ/kg·K)
λ	Air-Fuel Equivalence Ratio
ε	Exergy Efficiency

necessitating research to optimize their operation [10].

JP5, a kerosene-based aviation fuel, is widely used in military and maritime applications due to its high energy density and stability in changing environmental conditions [11,12]. Despite its advantages, the combustion of JP5 causes significant pollutant emissions, including carbon monoxide (CO), hydrocarbons (HC) and nitrogen oxides (NO_x), which are harmful to both the environment and human health [13]. As a result, there is growing interest in exploring alternative fuel mixtures and combustion improvement technologies to maintain or improve engine performance while reducing these emissions [14]. JP5 fuel exhibits a longer ignition delay compared to diesel fuel (DF), which is attributed to its excellent vaporization and low cetane number. This results in a shorter combustion time and higher heat release rates [13,15]. JP5 fuel creates higher oxygen (O_2) and lower carbon dioxide (CO_2) compared to diesel fuel. However, it produces higher levels of nitrogen oxide (NO_x) due to large heat release during combustion [16]. Although JP5 fuel is primarily designed for jet engines, it appears to exhibit different combustion characteristics compared to diesel fuel, such as longer ignition delay and higher heat release rates [17]. Fuels developed to mimic JP5 have shown promising results in various engine tests, closely matching the performance of the real fuel [18]. Using JP5 fuel in a spark ignition engine increases knock intensity and power loss at mid to high throttle openings compared to gasoline. Lowering the compression ratio reduces knock and can improve brake power (BP) and brake thermal efficiency (BTE) at certain throttle openings. At a compression ratio of 7.2, HC emissions are higher, while CO and NO emissions are lower compared to gasoline. Reducing the compression ratio reduces HC and NO emissions while increasing CO emissions [19]. These studies indicate that although JP5 can be used in spark ignition engines, its unique properties and emissions profile must be carefully managed.

A promising approach is the integration of HHO (Oxyhydrogen) generators with conventional fuels. HHO gas produced through the electrolysis of water contains a stoichiometric ratio of hydrogen and oxygen, which can be introduced into the combustion chamber to support a more complete and efficient combustion process. It has been reported that the addition of HHO gas improves combustion properties, reduces specific fuel consumption, and reduces the emission of harmful pollutants. Studies have shown a fuel consumption reduction of 14.8% and 16.3% for 150 cc and 1300 cc engines, respectively [20]. Another study reported a 20–30% reduction in fuel consumption on a 197 cc single-cylinder engine [21]. The addition of HHO gas provides a significant reduction in harmful emissions. For example, one study reported that CO emissions decreased by 24.5% and 33%, and HC emissions decreased by 21% and 27.4% for 1300 cc and 150 cc engines, respectively [20]. Another study reported that CO emissions can be reduced by approximately 98% under idling conditions [22]. Additionally, it appears that there have been studies reporting that HHO gas reduces CO and HC emissions in various passenger cars [23,24]. However, it seems that the effects of combining HHO with JP5 have not been sufficiently investigated, especially in 2-stroke spark ignition engines used in UAVs. Studies have reported that the use of HHO gas in internal combustion engines can improve engine performance by increasing combustion efficiency. However, it has been reported that excessive HHO flow at low engine speeds may negatively affect engine torque and volumetric efficiency [25]. It has been reported that the use of HHO gas in diesel engines reduces CO and HC emissions, although it increases CO_2 and NO_x emissions [26]. Several studies have shown that adding HHO gas to conventional fuels can lead to significant improvements in engine performance measurements. For example, the use of HHO gas in a spark-ignition engine has been shown to increase brake thermal efficiency and reduce specific fuel consumption (SFC) [27–29]. Studies show that the reason for the increase in engine efficiency is the high diffusivity of hydrogen and its rapid flame spread, contributing to more complete combustion [30–33]. The environmental benefits of using HHO gas as a fuel additive have been documented by research results [34]. Studies have consistently reported reductions in harmful emissions such as carbon monoxide (CO), hydrocarbons (HC), and smoke when HHO gas is used in combination with conventional fuels [35,36]. For example, one study found that adding HHO gas to a spark-ignition engine led to a 53% reduction in CO emissions and a 62% reduction in HC emissions [27]. Another study highlighted a 10.59% reduction in NO_x emissions when using an HHO-CNG blend compared to gasoline [28].

Despite promising results, there are challenges associated with the use of HHO gas in internal combustion engines [37]. A major issue is the energy required for onboard HHO production by electrolysis, which necessitates using some of the efficiency gains for electrolysis [38]. Additionally, the high reactivity of hydrogen leads to increased NO_x emissions due to higher combustion temperatures [39–41]. Proper management of HHO flow rates is an important issue to prevent negative effects on engine torque and volumetric efficiency, especially at low engine speeds [42].

Integration of HHO gas generators with JP5 fuel in spark ignition engines offers promising improvements in engine performance and emissions reductions. This study investigated the effects of using JP5 and HHO gas mixtures on the performance and exhaust emissions of a two-stroke, two-cylinder, air-cooled UAV engine. Experiments were conducted under various engine loads and speeds to comprehensively evaluate the effect of HHO integration on key performance parameters such as exhaust temperature, exhaust emissions and fuel consumption. By providing data on the potential benefits and drawbacks of this fuel combination, this research will contribute to ongoing efforts to develop

more efficient and environmentally friendly propulsion systems for UAVs. Table 1 shows a comparison of similar studies.

1.1. Research gap and Innovation

The presented study addresses a significant research gap in the field of dual-fuel UAV engines, particularly with respect to the application of Hydroxy gas (HHO) with JP5 aviation fuel. While existing research has focused heavily on the energy performance and environmental impacts of conventional aviation fuels and some alternative fuels, the use of HHO gas in UAV engines has not yet been explored. This study examines the energy, exergy, exergoenvironmental and exergoeconomic impacts of this novel fuel combination in a two-stroke UAV engine, providing valuable insights into its potential for cleaner and more efficient aviation propulsion systems.

1.2. Novelty and need of this study

- **Unexplored HHO Gas Application:** Since previous studies have lacked the investigation of Hydroxy gas (HHO) as a green fuel additive in two-stroke UAV engines, its performance and environmental impacts have not been sufficiently investigated.
- **Initial Energy and Exergy Analysis:** This is the first study to evaluate the combined energy, exergy, exergoenvironmental and exergoeconomic aspects of a UAV engine using JP5+HHO, providing an in-depth thermodynamic assessment.
- **Fuel Efficiency Improvements:** Significant improvements in engine performance are highlighted, showing a 10% reduction in Brake Specific Fuel Consumption (BSFC) and a 10% increase in exergy efficiency with the JP5+HHO blend.
- **Reduction of Exergy Destruction:** The study demonstrates a new 10% reduction in exergy destruction, previously unexplored in similar installations.
- **Comprehensive Impact Assessment:** The study provides a holistic perspective by not only focusing on energy performance, but also integrating environmental and economic impacts, which are rarely considered together in similar studies.
- **Sustainability in UAV Engines:** By demonstrating the potential of HHO as a renewable fuel source, this study contributes to the development of sustainable aviation fuels, which is essential to reduce environmental impacts in UAV applications.

This research provides much-needed insight into how HHO as a green fuel additive can improve the efficiency and sustainability of UAV engines. It fills an important gap in the literature and provides a path for future developments in green aviation technologies.

2. Material and methods

2.1. Engine setup

The experiments were carried out in the R&D laboratory of Erin Motor Company. The experimental engine is a two-stroke two-cylinder engine developed for UAV. The technical specifications of the engine are

Table 2
Test engine properties.

Technical Specification	Value (unit)
Brand&Model	Erin Motor & Baykuş
Number of cylinders	2
Cooling type	Air cooled
BorexStroke	48x36.5 (mmxmm)
Total cylinder volume	0.132 (liter)
Maks. Power	12 Hp (@8000 rpm)
Compression ratio	10.4:1
Idle speed	1800 (rpm)
Recommended propeller Diameter	27 (Inch)

Table 1
Comparison table of our study with similar studies.

Study	Fuel Type	Engine Type	Key Focus	Novelty	Key Findings
This study	JP5 + HHO (Hydroxy gas)	Two-stroke UAV engine	Energy, exergy, exergoenvironmental, and exergoeconomic analysis	First study on the use of HHO in UAV engines; comprehensive thermodynamic and environmental assessment	10% reduction in BSFC
Combustion efficiency analysis and key emission parameters of a turboprop engine at various loads [43].https://doi.org/10.1016/J.JOEI.2014.09.010	Aviation fuel	Military turboprop engine	Combustion efficiency	The combustion efficiency of a military turboprop engine varies between 97.8% and 99.9%, with emission parameters proving their relationship and establishing the combustion efficiency relationship.	Combustion efficiency of the engine ranged from 97.8% to 99.9%.
Performance of a small-scale turbojet engine fed with traditional and alternative fuels[44]. https://doi.org/10.1016/J.ENCONMAN.2014.03.026	Jet A GTL (FSJF) Blend 70% Jet-A 30% JME JME (pure)	SR-30 turbojet	CO, UHC, and NO_x emissions	Three different fuels, a traditional Jet-A kerosene, a synthetic gas to liquid (GTL) fuel and a blend of 30% Jatropha methyl ester (JME) and 70% Jet-A, were tested. The experimental results, in term of CO, UHC and NO_x emissions, are discussed and compared with results obtained from CFD analysis and from semi-empirical equations found in literature.	The JME blend reduced CO and UHC emissions compared to Jet-A kerosene.
Turbocharging the aircraft two-stroke diesel engine [45] https://doi.org/10.19206/ce-2019-319	Diesel	Aircraft two-stroke diesel engine	Engine performance at high altitudes	A turbocharger with a mechanical compressor extends high-altitude operating range.	Turbocharging an aircraft two-stroke diesel engine with a mechanical compressor extends its operating range at high altitudes, improving power and efficiency.
Combustion and emission characteristics from biojet fuel blends in a gas turbine combustor [46] https://doi.org/10.1016/j.energy.2019.06.060	Jet A1 + Biofuels (BF) derived from Jatropha and Camelina	Gas turbine	Combustion efficiency, temperature rise, emission indices.	Addition of biodiesel to jet A1 fuel in gas turbine for aviation engine	Increasing Camelina in biojet fuel blends reduces carbon monoxide, unburnt hydrocarbons, and soot emissions, but increases NO_x emissions due to higher combustion temperatures.

given in Table 2.

The engine tests were carried out in the engine test laboratory of Erin Motor Company with sound insulated cabinets (see Table 3). The propeller thrust of the test engine is measured with an 'S' type load cell and the engine torque is calculated. The consumption time of a fixed 20 mL volume of fuel is measured in seconds with a stopwatch and the fuel consumption is calculated with the value obtained. Engine speed is measured with a laser tachograph meter from a point on the propeller. Engine casing temperature was determined with a thermal camera and exhaust gas temperature was determined with a K-type thermocouple. Exhaust gas emissions were measured with BOSCH-BEA 060 brand emission measuring device (Fig. 1).

The engine was tested using two different fuel configurations: 100% JP5 and HHO gas produced from an internal HHO generator supplied through the intake manifold at flow rates of 1, 1.5, 2 and 4 liters/min. The HHO generator produces oxyhydrogen gas by electrolysis of water. The HHO gas used in the engine experiments was produced in the HHO generator per hour consisting of 30 titanium pieces cut in 60 cm × 40 cm dimensions. The HHO generator has been determined how many liters of gas it produces in which current range with preliminary trials. In the preliminary trials, it was seen that the HHO generator could produce 25 L of gas per hour. Before the engine experiments, a 10 L tank was placed in the front compartment of the HHO generator. The amount of gas sent to the engine could be adjusted by means of a flowmeter controlled through a ball valve. The physical properties of JP5 fuel and HHO gas used in the experiments are given in the table below.

2.1.1. Evaluation of test fuels in terms of cetane number

JP5 is a kerosene-type aviation fuel, so it typically has a cetane number around 45–50. The cetane number of JP5 indicates its ignition quality. A higher cetane number means the fuel has a shorter ignition delay, resulting in smoother and more efficient combustion in compression ignition engines such as diesel engines. Although JP5 is primarily used in turbine engines, the cetane number is important for evaluating combustion characteristics in dual-fuel modes in diesel engines. Hydrogen has no cetane number because it does not behave like traditional liquid fuels. It is a gaseous fuel with a very high autoignition temperature (~585 °C) and lacks the typical ignition delay properties measured by the cetane number. Hydrogen is highly reactive and burns faster than hydrocarbon fuels. Despite its lack of cetane number, its rapid flame propagation makes it suitable for use as an additive in spark ignition engines or dual-fuel systems, where it can increase combustion efficiency and reduce emissions.

2.2. Test conditions

Engine performance and exhaust emissions were evaluated at various engine loads and speeds to simulate typical operating conditions of UAVs. Engine Speeds and Loads: 5 kg at 3250 rpm, 10 kg at 3750 rpm, 15 kg at 4500 rpm, 20 kg at 5250 rpm, and 25 kg at 6250 rpm. Engine speed was measured with a point laser tachograph meter attached to the engine output shaft. It was measured with an S-type load cell connected to the dynamometer arm. Exhaust gas temperature was measured with a thermocouple placed at the exhaust outlet. The engine casing temperature was measured with a thermal imaging camera placed permanently in front of the engine. The consumption time of 20 ml of fuel was measured in seconds with a stopwatch. An exhaust gas analyser was used to determine the concentrations of CO, HC, NO_x, CO_2, O_2 and lambda. Humidity, pressure and temperature values in the experimental area were measured to ensure that the experiments were carried out under standard conditions (Table 4). The measurement ranges of all sensors used in the experimental setup and the uncertainty analysis of the whole system are given in Table 5.

The engine was mounted on a test bench equipped with the necessary instrumentation to measure performance and emissions. The fuel system was configured to allow switching between pure JP5 and a JP5+HHO mixture. The engine was initially run at 100% JP5 to establish baseline performance and emissions data across the specified engine speeds and loads. The HHO generator was activated and the generated Oxyhydrogen gas was introduced into the engine intake manifold. The engine was then run with a JP5+HHO mixture under the same test conditions. At each engine speed and load, data on exhaust temperature, emissions, and fuel consumption were recorded. Each test was repeated three times to ensure repeatability and accuracy of the results. This study aims to

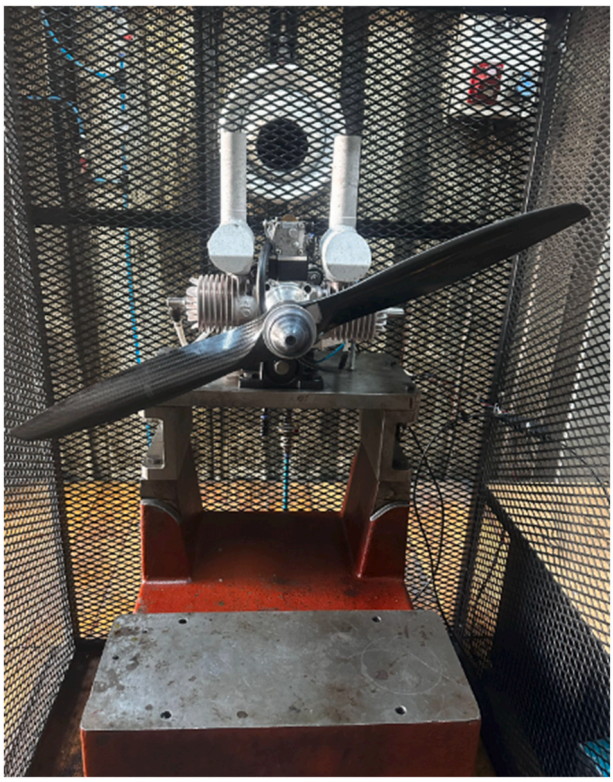

Fig. 1. Experimental engine and test unit.

Table 3
Properties of test fuels [47].

Properties/Test Fuel	JP5	HHO
Density @ 15 °C, kg/L	0.8145	0.00008988
Distillation, °C	240	–
Sulfur content, wt%	0.0110	–
Flash point, °C	68	–
Kinematic viscosity, cSt, (20 °C)	5.39	8.76
Cetane index	44	–
Cetane number	50	–
Freezing point, °C	−50	Hydrogen has a freezing point of −259.16 °C, and oxygen has a freezing point of −218.79 °C.
Aromatics, vol%	16.83	–
Lower heating value, MJ/kg	43.2	10.8

Table 4
Exhaust gas Emission device.

Measurement	Measuring Range	Resolution
CO	0-10 vol %	0.001 vol%
CO_2	0-18 vol%	0.10 vol%
HC	0–9,999 ppm	1.0 ppm
O_2	0-22 vol%	0.10 vol%
NO_x	0–5000 ppm	1.0 ppm

Table 5
Equipment used in the experimental setup.

Measurement	Measuring Range	Resolution
Temperature	K type (0–1400 °C)	0.1 °C
Engine speed	2.5–99,999 rpm	1 rpm
Thermal camera	−10 – 1000 °C	±2 °C
Fuel measurement	10–1000 mL	0.1 vol%
Flowmeter	0-100 L/min	±2 %

systematically evaluate the effects of HHO integration on a two-stroke spark ignition UAV engine, providing valuable information on potential performance improvements and emission reductions that can be achieved using alternative fuel technologies.

Table 6 illustrates the precision of the measuring instruments used during the tests. For each parameter measured (such as engine speed, fuel consumption, temperature, and emissions), the instruments possess a defined range of measurement and a corresponding level of accuracy, known as uncertainty. These uncertainties indicate the potential deviation of the results from the true values, thereby providing a measure of confidence in the obtained data. The engine speed was recorded using a tachograph meter capable of measuring within a range of 2.5–99,999 revolutions per minute (rpm), with a resolution of 1 rpm. However, due to the inherent variability in multiple readings, an additional uncertainty of 0.5% of the measured speed was introduced. Propeller thrust was determined via a load cell, which measures force with a precision of 0.01 kg. The load cell also exhibited a calibration-related uncertainty of 0.1%. Torque, a measure of rotational force, was not directly measured but rather calculated from the thrust. As a result, any uncertainty in thrust measurements contributes to the uncertainty in the torque calculations. Fuel consumption was assessed by timing the duration required to consume a fixed 20 mL volume of fuel, using a stopwatch with a precision of 0.1 s. Additionally, the fuel volume was measured with an accuracy of 0.1 mL. The combination of these uncertainties contributes to the total uncertainty in fuel consumption.The temperature of the engine casing was measured using a thermal camera, which is capable of recording temperatures between −10 °C and 1000 °C, with an accuracy of ±2 °C. This implies that the recorded temperature could deviate by up to 2 °C in either direction. Exhaust gas temperatures were determined using a highly accurate K-type thermocouple, with a precision of ±0.1 °C. Emissions were measured using a BOSCH-BEA 060 gas analyzer. Carbon monoxide (CO) levels were detected within the range of 0–10 vol%, with a resolution of 0.001 vol%. The same analyzer measured carbon dioxide (CO_2) concentrations between 0 and 18 vol%, with a precision of ±0.10 vol%. Hydrocarbons (HC) were measured in parts per million (ppm), with the analyzer capable of detecting levels between 0 and 9999 ppm, and a resolution of ±1.0 ppm. Oxygen (O_2) concentrations were measured within the range of 0–22 vol%, with a precision of ±0.10 vol%. Finally, nitrogen oxides (NO_x) emissions were measured within the range of 0–5000 ppm, with a precision of ±1.0 ppm (see Fig. 2).

2.3. Energy and exergy analysis

The current study focuses on the performance, energy, exergy, exergoenvironmental and exergoenvironmental impacts of JP5 aviation fuel and JP5+HHO dual fuel combustion of a two-stroke, air-cooled, UAV engine. Before starting thermodynamic calculations, it is assumed that the engine operates steadily, the exhaust gases and the air entering the intake manifold are ideal gases, and the combustion gases are in chemical equilibrium. Additionally, to facilitate thermodynamic analyses, it is assumed that the control volume (CV) of the engine is an open system and that kinetic and potential changes of inflows and outflows are neglected [48,49]. The ambient temperature is assumed to be 15.4 °C, and the ambient pressure is 99.7 kPa during the analyses. As seen in Fig. 3, the energies entering and exiting the two-stroke air-cooled UAV engine to which thermodynamic analysis will be applied represent the CV.

According to the 1st law of thermodynamics, the total energies entering and exiting CV are equal to each other and are indicated by Eq. (1) [50].

$$\sum Ene_{in} = \sum Ene_{out} \tag{1}$$

In the engine system, the energy input consists of the air and fuel energies, while the output energies include shaft work ($\dot{S}_{work}$), exhaust ($\dot{E}ne_{exh}$), and losses ($\dot{E}ne_{lost}$). The unit of all these energy flows is kW. Assuming the temperature of the intake air entering the system remains unchanged, the fuel energy equals the sum of shaft work, exhaust, and loss energies, as seen in Eq. (2) [51].

$$\dot{E}ne_{fuel} = \dot{S}_{work} + \dot{E}ne_{exh} + \dot{E}ne_{lost} \tag{2}$$

Eq. (3) can be used to determine the fuel energy of a engine operated at different shaft speeds [52]. Where $\dot{m}_{fuel}$ represents the mass flow rate of the fuel in kg/s, while LHV_{fuel} represents the lower heating value of the fuel in kJ/kg.

$$\dot{E}ne_{fuel} = \dot{m}_{fuel} LHV_{fuel} \tag{3}$$

As seen in Eq. (4), the torque value of the engine ($Torque_{JE}$, Nm) can be calculated by taking into account the thrust force (F_{trust}) measured during the experiments (49 N, 98 N, 147 N, 196 N and 245 N) and the thrust arm length (X) (0.0365 m). In order to determine the shaft work of the engine, the shaft speed and the calculated torque value are taken into account and can be calculated using equation (5) [53].

$$Torque_{JE} = F_{trust} X \tag{4}$$

$$\dot{S}_{work} = 2\pi \frac{n \,.\, Torque_{JE}}{60} \tag{5}$$

Eq. (6) can be used to calculate the $\dot{E}ne_{exh}$ coming out of the CV. Where m_i represents the mass flow rate of the combustion gas at state i in kg/s, while h_i represents the specific enthalpy of the burned gas at state i in kJ/kg.

Table 6
Uncertainty analyses for equipment.

Measurement	Instrument	Range	ResolutIon	UncertaInty
Engine speed	Laser tachograph meter	2.5–99,999 rpm	1 rpm	±1 rpm + ±0.5%
Propeller thrust	'S' type load cell	As per specs	±0.01 kg	±0.1% calibration + ±0.01 kg resolution
Fuel consumption	Stopwatch and volume	Manual measurement	±0.1 s, ±0.1 ml	±0.1 s, ±0.1 ml
Engine casing temperature	Thermal camera	−10 °C–1,000 °C	±2 °C	±2 °C
Exhaust gas temperature	K-type thermocouple	0–1400 °C	±0.1 °C	±0.1 °C
CO emission	BOSCH-BEA 060	0-10 vol%	±0.001 vol%	±0.001 vol%
CO_2 emission	BOSCH-BEA 060	0-18 vol%	±0.10 vol%	±0.10 vol%
HC emission	BOSCH-BEA 060	0–9,999 ppm	±1.0 ppm	±1.0 ppm
O_2 emission	BOSCH-BEA 060	0-22 vol%	±0.10 vol%	±0.10 vol%
NO_x emission	BOSCH-BEA 060	0–5,000 ppm	±1.0 ppm	±1.0 ppm

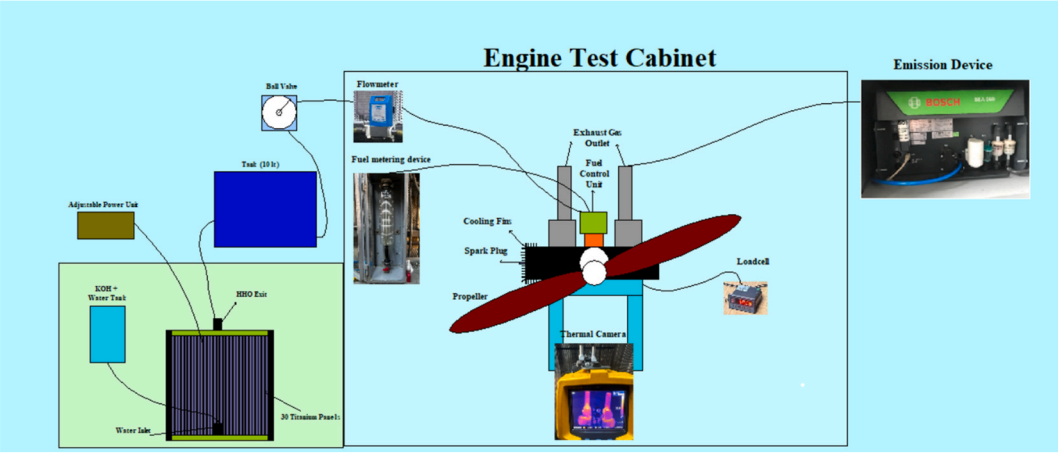

Fig. 2. Schematic view of the test setup.

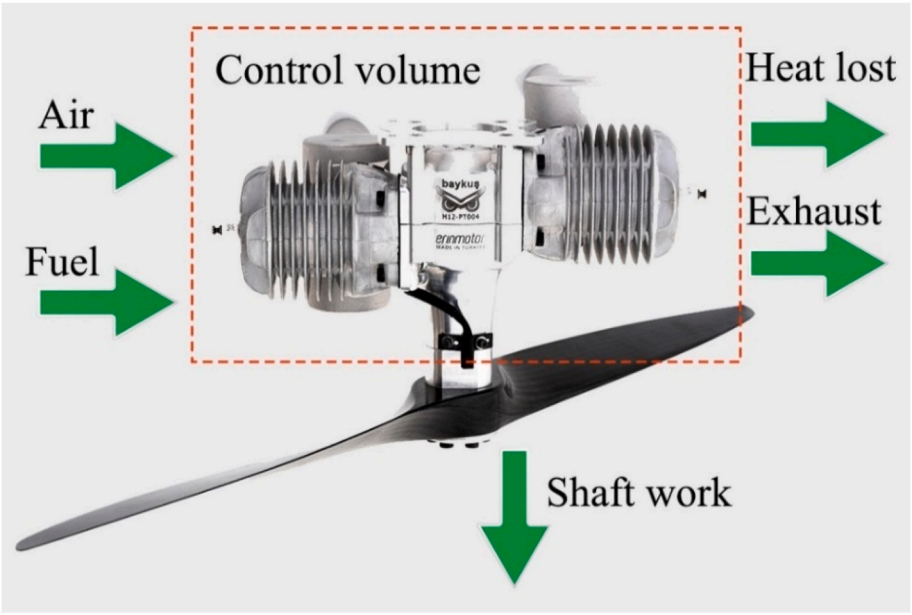

Fig. 3. Schematic view of CV for energy and exergy evaluation of two-stroke air-cooled UAV engine.

$$\dot{E}ne_{exh} = \sum_{i=1}^{n} m_i x h_i = m_{CO2} h_{CO2} m_{H2O} h_{H2O} + m_{CO} h_{CO} \ldots \quad (6)$$

The lost energy from the control volume of the engine can be calculated using equation (7).

$$\dot{E}ne_{lost} = \dot{E}ne_{fuel} - [\dot{S}_{work} + \dot{E}ne_{exh}] \quad (7)$$

When the shaft work of a engine is divided by the fuel energy consumed, the energy efficiency is obtained, as shown in Eq. (8).

$$Energy\ efficiency = \frac{\dot{S}_{work}}{\dot{E}ne_{fuel}} \quad (8)$$

Exergy defines what energy degradation means and is also an indicator of how much useful work can be achieved from available fuel energy. Eq. (9) expresses the exergy balance according to the 2nd law of thermodynamics. Where $\dot{E}xe_{in}$ and $\dot{E}xe_{out}$ refer to the incoming and outgoing exergy flows, while $\dot{E}xe_{Dest}$ refers to the destroyed exergy ($\dot{E}xe_{Dest}$).

$$\dot{E}xe_{in} = \dot{E}xe_{out} + \dot{E}xe_{Dest} \quad (9)$$

As seen in Eq. (10), while the exergy entering the CV is fuel exergy ($\dot{E}xe_{fuel}$), the exergy leaving the CV is exergy power ($=\dot{S}_{work}$) [54], exhaust exergy($\dot{E}xe_{Exh}$), heat transfer exergy($\dot{E}xe_{Heat}$), and exergy destroyed($\dot{E}xe_{Dest}$), respectively.

$$\dot{E}xe_{fuel} = \dot{S}_{work} + \dot{E}xe_{Exh} + \dot{E}xe_{Heat} + \dot{E}xe_{Dest} \quad (10)$$

The $\dot{E}xe_{fuel}$ of the system is obtained by multiplying the fuel energy ($\dot{m}_{fuel}\ x\ LHV_{fuel}$) and the chemical exergy factor (φ_{fuel}) and can be calculated as seen in Eq. (11). Additionally, the φ_{fuel} can be calculated according to the compound mass ratios (a = h/c, b = o/c, and c = s/c) of the fuel mixtures, as can be seen in Eq. (12) [55].

$$\dot{E}xe_{fuel} = \dot{m}_{fuel}\ LHV_{fuel}\ \varphi_{fuel} \quad (11)$$

$$\varphi_{fuel} = 1.0401 + 0.1728\ a + 0.0432\ b + 0.2169\ c(1 - 2.0628a) \quad (12)$$

The $\dot{E}xe_{Exh}$ coming out of the engine CV is a function of the mass flow rate (at state i) of the combustion products and the combustion gases, and is obtained by multiplying these two functions as in Eq. (13) [56].

$$\dot{E}xe_{Exh} = \sum_{i=1}^{n} \dot{m}_i \left[e_{tm,i} + e_{ch,i} \right] \tag{13}$$

$e_{tm,i}$ symbolizes the thermochemical specific exergy and $e_{ch,i}$ symbolizes the chemical specific exergy of the combustion products. $e_{tm,i}$ and $e_{ch,i}$ are calculated with Eq. (14) and Eq. (15), respectively [57].

$$e_{tm,i} = \sum_{i=1}^{n} \left[\left(\overline{h}_i - \overline{h}_{i,0} \right) - T_0 \left(\overline{s}_i - \overline{s}_{i,0} \right) \right] \tag{14}$$

$$e_{ch,i} = \overline{R} T_0 \sum_{i=1}^{n} \left[ln \frac{e_{env,i}}{e_{exh,i}} \right] \tag{15}$$

In Eq. (14), $\overline{h}$ symbolizes molar enthalpy and $\overline{s}$ symbolizes molar entropy. In Eq. (15), $\overline{R}$ symbolizes the specific gas constant and T_0 symbolizes the reference temperature. Also, $e_{exh,i}$ symbolizes the molar ratio of the exhaust gas compound in case i, and $e_{env,i}$ symbolizes the molar ratio of compound i in the reference environment [58].

The heat transfer exergy occurring from the two-stroke air-cooled engine surface to the surrounding environment can be calculated with Eq. (16) [59]. Here T_s denotes the engine surface temperature.

$$\dot{E}xe_{Heat} = \sum \dot{E}ne_{lost} \left[1 - \frac{T_0}{T_s} \right] \tag{16}$$

By proportioning the engine shaft work to the fuel exergy, exergy efficiency can be obtained as seen in Eq. (17).

$$Exergy\ efficiency = \frac{\dot{S}_{work}}{\dot{E}xe_{fuel}} \tag{17}$$

Irreversibility that occurs during the operation of the engine can be calculated with Eq. (18) [60].

$$\text{Irreversibility} = \frac{\dot{E}xe_{Dest}}{T_0} \tag{18a}$$

2.4. Exergoenviromental and exergoenviroeconomic analysis

In this experimental study, the amount of CO_2 emitted into the environment as a result of combustion of a two-stroke, air-cooled UAV engine is used for exergoenvironmental and exergoeconomic analysis evaluations. In exergoenvironmental analysis calculations, as shown in Eq. (19), the CO_2 emissions released into the environment over the course of one year (Exe_{evn}) are considered, including calculations for CO_2 emitted per unit of engine power ($\dot{m}_{env}\dot{S}_{work}$) and the engine's operational duration (h_{ope}) [61,62]. As a result of the exergoenvironmental analysis, the amount of CO_2 released into the surrounding environment (ton CO_2/year) by operating the engine 8 h a day at the end of one year (330 days) is determined [63].

$$Exe_{evn} = \dot{m}_{evn} \dot{S}_{work} h_{ope} \tag{18b}$$

$$Exe_{eco} = Exe_{env}\ ec_{CO2} \tag{19}$$

Eq. (19) can be utilized for exergoenviroeconomic (Exe_{eco}) analysis calculations [64]. In this equation, ec_{CO2} represents the cost of CO_2, and for the calculations, the average CO_2 cost for the year 2023 is accepted to be 78.23 Euros [65].

3. Results and discussion

Experiments are conducted on a small UAV two-stroke engine fueled by JP5, operating at various engine shaft speeds (ranging from 3250 rpm to 6250 rpm) and in dual-fuel mode (JP5-HHO gas). The thrust loads corresponding to the engine shaft speeds of 3250, 3750, 4500, 5250, and 6250 rpm are measured as 49, 98, 147, 196, and 245 N, respectively. In these experiments, HHO gas is injected into the engine cylinder in addition to JP5 fuel, at different mass flow rates (1, 1.5, 2, and 4 L per minute (lpm)). Data obtained from the experiments are used to analyze engine performance, emissions, energy, exergy, exergoenvironmental impact, and exergoenviroeconomic factors, which are presented in this section.

3.1. Performance and emissions

In Fig. 4, torque and shaft work of the engine are presented for different shaft speeds. Additionally, Fig. 4 displays brake specific fuel consumptions (BSFC) of JP5, JP5+HHO 1, JP5+HHO 1.5, JP5+HHO 2, and JP5+HHO 4 fuels at various shaft speeds. In the current experimental parameters, torque and shaft work of the engine increase with increasing shaft speed from 3250 to 6250 rpm. The highest torque and shaft work values are achieved at 6250 rpm, measuring 8.95 Nm and 5.86 kW, respectively. BSFC values for test fuels show the highest values at 3250 rpm and the lowest values (excluding JP5) at 6250 rpm. For instance, at 3250 rpm, JP5 fuel exhibits a BSFC value of 2038.6 g/kWh, while the BSFC values for the engine operated in dual-fuel mode with 1, 1.5, 2, and 4 lpm HHO gas show reductions of 6.9%, 9.6%, 9.6%, and 11.5%, respectively. Similarly, at the lowest BSFC values observed at 6250 rpm, JP5 fuel shows a BSFC of 562.6 g/kWh, whereas the BSFC values for the engine operated in dual-fuel mode with 1, 1.5, 2, and 4 lpm HHO gas show reductions of 9.8%, 14.1%, 11.1%, and 15.1%, respectively. Overall, compared to JP5 fuel across the 3250–6250 rpm range, the average reductions in BSFC are approximately 6.3%, 9.4%, 7.8%, and 10.9%, respectively. Compared to JP5 fuel, one of the significant reasons for the reduced fuel consumption when using HHO is its ability to create a homogeneous mixture in the air intake and increase the combustible oxygen content. Hydrogen is a fuel with high combustion capacity, and it demonstrates this ability within HHO. This leads to the creation of better combustion conditions, resulting in lower BSFC. The results obtained on BSFC are in line with studies that have achieved a reduction in BSFC with the use of HHO [21,25]. Additionally, the gradual increase of HHO gas in dual-fuel applications, leading to a reduction in BSFC, was also reported by Kenanoğlu et al. [42].

Fig. 5 displays exhaust gas temperature (EGT) of JP5, JP5+HHO 1, JP5+HHO 1.5, JP5+HHO 2, and JP5+HHO 4 fuels at various shaft speeds. As the shaft speed increases from 3250 rpm to 6250 rpm, the EGT of all test fuels increase. The reason for this is the increase in the total mass flow rate into the cylinder with higher speeds, which prolongs the combustion process. The lowest EGT for all test fuels is observed at 3250 rpm, while the highest EGT is observed at 6250 rpm. For instance, at 3250 rpm, JP5 fuel exhibits an EGT value of 346 K, while the EGT values for the engine operated in dual-fuel mode with 1, 1.5, 2, and 4 lpm HHO gas show increases of 0.6%, 1.4%, 2.3%, and 1.2%, respectively. Similarly, at the highest EGT values observed at 6250 rpm, JP5 fuel shows an EGT of 382 K, whereas the EGT values for the engine operated in dual-fuel mode with 1, 1.5, 2, and 4 lpm HHO gas show increases of 1.6%, 2.1%, 2.6%, and 1%, respectively. Overall, compared to JP5 fuel across the 3250–6250 rpm range, the average increases in EGT are approximately 1%, 1.5%, 2%, and 1%, respectively. Generally, across all speeds, JP5 fuel exhibits the lowest EGT, whereas operating with dual-fuel mode including HHO additives results in increased EGT values. The reason for this can be attributed to HHO gas improving the combustion process and simultaneously increasing the gas temperatures due to the presence of H_2 (hydrogen). Similarly, the engine surface temperature (EST) tends to increase with the increase in shaft speed. Additionally, the use of HHO as an additional dual fuel with JP5 fuel also contributes to the increase in ESTs. The lowest EST for all test fuels is observed at 3250 rpm, while the highest EST is observed at 6250 rpm. For instance, at 3250 rpm, JP5 fuel exhibits an EST value of 328 K, while the EST values for the engine operated in dual-fuel mode with 1, 1.5, 2, and 4 lpm HHO gas show 329 K, 331 K, 332 K, and 330 K, respectively. Similarly, at the highest EST values observed at 6250 rpm, JP5 fuel shows an EST of 371 K, whereas the EST values for the engine operated in dual-fuel mode with 1, 1.5, 2, and 4 lpm HHO gas show 374 K, 376 K,

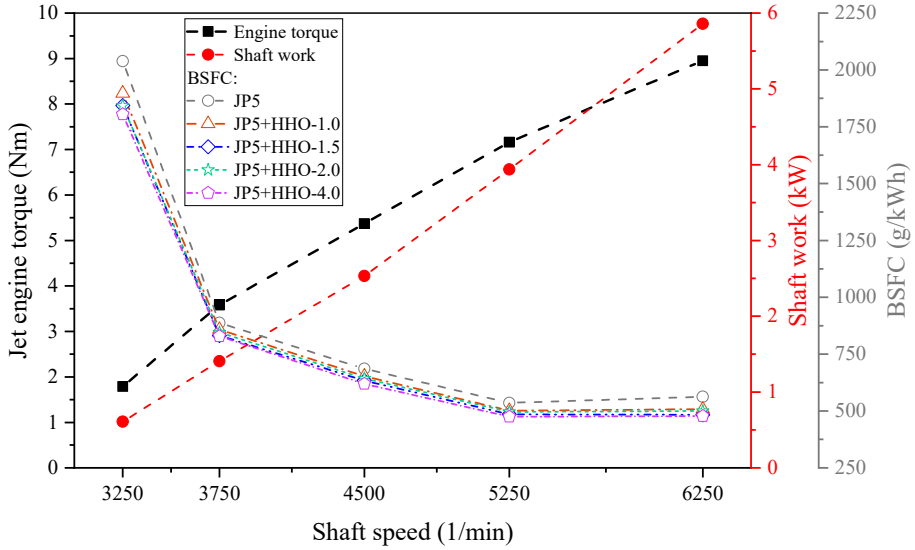

Fig. 4. Variation of torque, shaft work and BSFC of a two-stroke UAV engine at different shaft speeds.

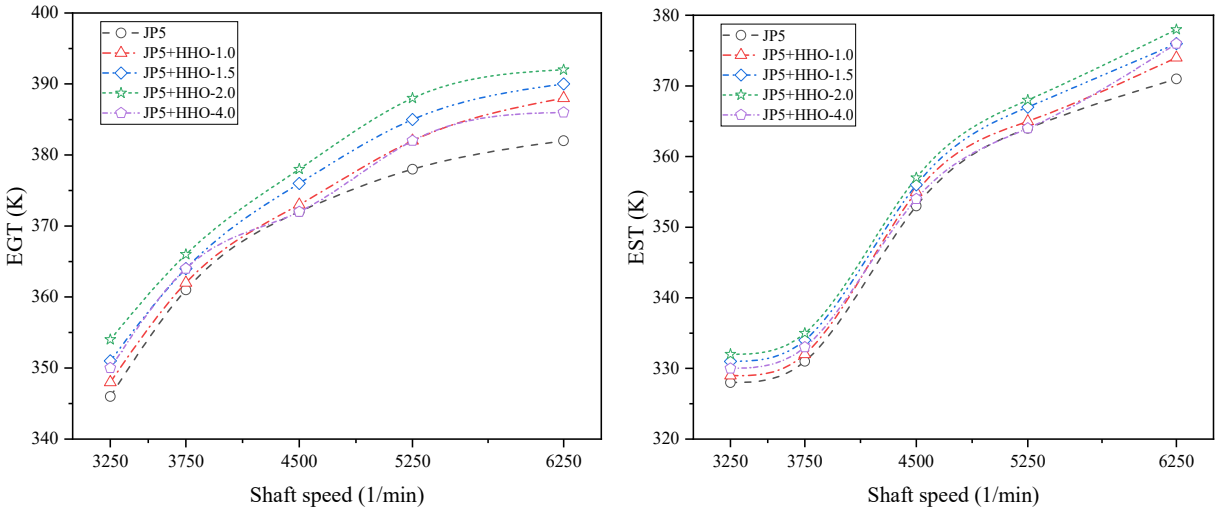

Fig. 5. Variation of EGT and EST of a two-stroke UAV engine at different shaft speeds.

378 K, and 376 K, respectively. Overall, compared to JP5 fuel across the 3250–6250 rpm range, the average increases in EST are approximately 0.5%, 1%, 1.3%, and 0.6%, respectively.

Fig. 6 (a) displays HC emission variation of JP5, JP5+HHO 1, JP5+HHO 1.5, JP5+HHO 2, and JP5+HHO 4 fuels at various shaft speeds. With the increase in shaft speed from 3250 to 6250 rpm, the HC emissions of all test fuels show a decreasing trend up to 5250 rpm. However, with the increase in shaft speed from 5250 to 6250 rpm, HC emissions tend to increase again. The most significant reason for this can be attributed to rapidly decreasing volumetric efficiency with increasing speed, as well as frictional forces. To overcome existing frictional forces, higher mass fuel consumption may contribute to an increase in HC emissions. The highest HC emissions for all test fuels are observed at 3250 rpm, while the lowest HC emissions are obtained at 5250 rpm. For instance, at 3250 rpm, the HC emissions for JP5, JP5+HHO 1, JP5+HHO 1.5, JP5+HHO 2, and JP5+HHO 4 fuels are 16.2 g/kWh, 17.2 g/kWh, 17.5 g/kWh, 17.8 g/kWh, and 18.7 g/kWh, respectively. At the shaft speed of 5250 rpm, which shows the lowest HC emissions, they are 7.3 g/kWh, 7.5 g/kWh, 7.8 g/kWh, 7.9 g/kWh, and 8.3 g/kWh. In a two-stroke engine, the use of JP5-HHO dual fuel results in increased HC emissions compared to JP5 fuel. Parameters such as the shape of the combustion chamber, valve timing, exhaust valve opening, intake mixture, and in-cylinder fluid dynamics can contribute to the formation of HC emissions [66]. The increase in O_2 content due to the presence of HHO gas in the combustion zone is expected to reduce HC emissions. However, in a two-stroke engine, while exhaust gases are expelled after combustion, the intake port simultaneously opens, allowing fresh charge to enter the cylinder. As a result, the prolonged opening of the exhaust port can cause some of the intake charge to escape, leading to an increase in HC emissions. Overall, compared to JP5 fuel across the 3250–6250 rpm range, the average increases in HC emission are approximately 4%, 6%, 8%, and 14%, respectively.

Fig. 6 (b) displays CO emission variation of JP5, JP5+HHO 1, JP5+HHO 1.5, JP5+HHO 2, and JP5+HHO 4 fuels at various shaft speeds. At all test speeds, the highest CO emissions are obtained with JP5 fuel, while the lowest CO emissions are achieved with JP5+HHO 2 dual fuel. For instance, at 3250 shaft speed, CO emissions with JP5 fuel are 293 g/kWh, whereas with JP5+HHO 2 fuel, CO emissions are 283 g/kWh. At 6250 shaft speed, CO emissions with JP5 fuel are 184 g/kWh, whereas with JP5+HHO 2 fuel, CO emissions are 171 g/kWh. The oxidation of carbon (C) in the fuel to CO_2 requires sufficient temperature and O_2. Otherwise, the C in the fuel is released as CO emissions instead

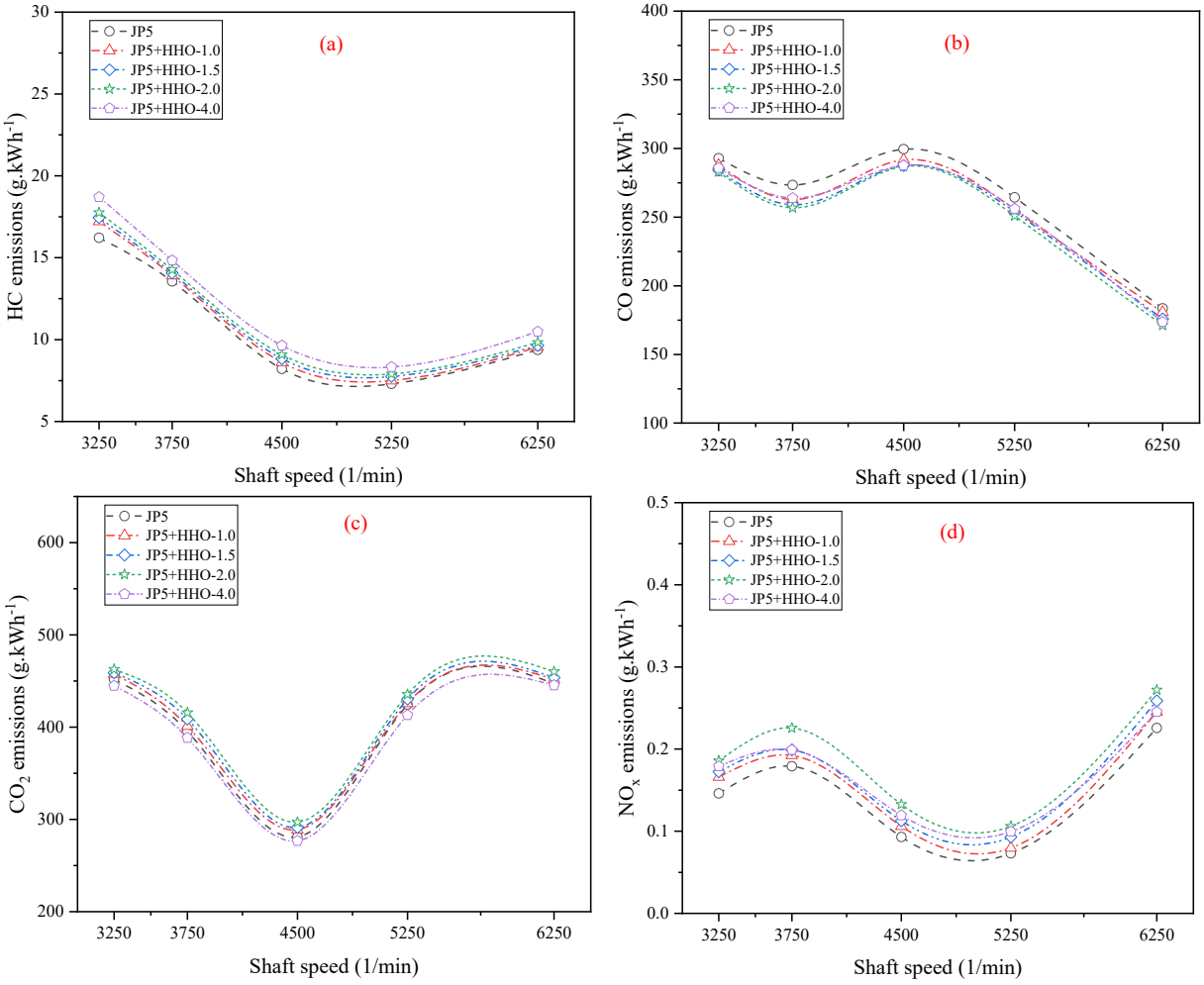

Fig. 6. (a)HC, (b)CO, (c)CO_2, and (d)NO_x emission variation of engine at different shaft speeds.

of CO_2 emissions [67]. In this dual-fuel application, HHO's ability to distribute evenly and increase the O_2 content in the combustion zone contributes to reducing CO emissions. Additionally, increased surface temperatures may lead to higher cylinder temperatures. In this scenario, elevated combustion temperatures also aid in reducing CO emissions. As seen in Fig. 6 (b), when CO emissions increase, CO_2 emissions decrease, and when CO emissions decrease, CO_2 emissions increase. Overall, JP5+HHO 1, JP5+HHO 1.5, JP5+HHO 2, and JP5+HHO 4 fuels compared to JP5 fuel across the 3250–6250 rpm range, the average reductions in CO emission are approximately 3%, 4%, 5%, and 4%, respectively.

Fig. 6 (c) displays CO_2 emission variation of JP5, JP5+HHO 1, JP5+HHO 1.5, JP5+HHO 2, and JP5+HHO 4 fuels at various shaft speeds. At shaft speeds of 3250 and 6250 rpm, the highest CO_2 emissions are obtained with JP5+HHO 2 fuel, while the lowest CO_2 emissions are achieved with JP5 and JP5+HHO 4 fuels. CO_2 emissions represent complete combustion products, suggesting that JP5+HHO 2 dual fuel achieves a higher combustion efficiency compared to other fuels based on these emission values. The delivery of HHO at 4 lpm may decrease volumetric efficiency and lead to poorer combustion conditions, potentially resulting in higher CO_2 emissions. Additionally, at 4500 rpm shaft speed where CO emissions peak, CO_2 emissions are at their minimum level, indicating that the conversion reactions from CO to CO_2 are halted, thus reducing CO_2 emissions. Overall, JP5+HHO 1, JP5+HHO 1.5, JP5+HHO 2, and JP5+HHO 4 fuels compared to JP5 fuel across the 3250–6250 rpm range, the average increases in CO_2 emission are approximately 1%, 2%, 4%, and −2%, respectively.

Fig. 6 (d) displays NO_x emission variation of JP5, JP5+HHO 1, JP5+HHO 1.5, JP5+HHO 2, and JP5+HHO 4 fuels at various shaft speeds. At shaft speeds of 3250 and 6250 rpm range, the highest NO_x emissions are obtained with JP5+HHO 2 fuel, while the lowest NO_x emissions are achieved with JP5. For instance, at 5250 shaft speed, NO_x emissions with JP5 fuel are 0.07 g/kWh, whereas with JP5+HHO 2 fuel, NO_x emissions are 0.11 g/kWh. At 6250 shaft speed, NO_x emissions with JP5 fuel are 0.23 g/kWh, whereas with JP5+HHO 2 fuel, NO_x emissions are 0.27 g/kWh. NO_x emissions are significantly formed under slightly lean air/fuel mixtures and high combustion temperatures [68]. In this study, the higher NO_x emissions at 2 L/min HHO gas compared to 4 L/min HHO gas can be explained as follows: Introducing more HHO gas into the cylinder (i.e., 4 L/min instead of 2 L/min) further lowers the lower heating value of the total fuel mixture. This reduction in combustion temperatures contributes to the decrease in NO_x emissions. Additionally, the excessive leaning of the combustion zone weakens the flame speed and slows down the combustion reactions, further reducing NO_x formation. Similar to the findings of this study, Kamarudin et al. [69] emphasized that NO_x emissions increase with the addition of HHO, but when the mixture becomes excessively lean or rich, NO_x emissions decrease due to the reduction in combustion temperatures. Overall, JP5+HHO 1, JP5+HHO 1.5, JP5+HHO 2, and JP5+HHO 4 fuels compared to JP5 fuel across the 3250–6250 rpm range, the average increases in NO_x emission are approximately 13%, 18%, 35%, and 23%, respectively. At high speeds, the increase in NO_x emissions may be attributed to the prolonged combustion duration caused by the increased fuel quantity delivered to meet high power and speed

demands. Additionally, the use of HHO can elevate combustion temperatures due to hydrogen's high flame speed and wide flammability range. This condition can also contribute to an increase in NO_x emissions, highlighting it as another factor contributing to their rise.

3.2. Energy analysis

Fig. 7 (a) displays fuel energy flows variation of JP5, JP5+HHO 1, JP5+HHO 1.5, JP5+HHO 2, and JP5+HHO 4 fuels at various shaft speeds. As shaft speed increases from 3250 to 6250 rpm, energy flow rates also increase. Meeting the increased shaft power requires more fuel injection, leading to an overall increase in total energy consumption. The lowest fuel energy flows are achieved at 3250 shaft speed, while the highest are at 6250 shaft speed. For example, at 3250 shaft speed, the fuel energy flow for JP5 fuel is 16.1 kW, whereas for JP5, JP5+HHO 1, JP5+HHO 1.5, JP5+HHO 2, and JP5+HHO 4 fuels, the respective fuel energy flows are 15.5 kW, 15.3 kW, 14.7 kW, and 14.6 kW. At 6250 shaft speed, JP5 fuel has a fuel energy flow of 42.6 kW, while JP5, JP5+HHO 1, JP5+HHO 1.5, JP5+HHO 2, and JP5+HHO 4 fuels have fuel energy flows of 41.9 kW, 39.8 kW, 38.1 kW, and 36.6 kW respectively. Overall, the dual-fuel application of JP5 fuel with HHO contributes to reducing the required energy amount to deliver the current power. This can be attributed to HHO's ability to distribute evenly inside the cylinder, its wide flammability range, and hydrogen's high flame speed, enhancing the combustion process. In the 3250 to 6250 shaft speed range, the average reductions in fuel energy flows compared to JP5 fuel are approximately 1%, 4%, 7%, and 9% for JP5, JP5+HHO 1, JP5+HHO 1.5, JP5+HHO 2, and JP5+HHO 4 fuels, respectively.

Fig. 7 (b) displays shaft work variation of JP5, JP5+HHO 1, JP5+HHO 1.5, JP5+HHO 2, and JP5+HHO 4 fuels at various shaft speeds. For all test fuels, shaft work increases as the shaft speed increases from 3250 to 6250 rpm: at 3250 shaft speed, 0.61 kW of shaft work is obtained; at 3750 shaft speed, 1.41 kW; at 4500 shaft speed, 2.54 kW; at 5250 shaft speed, 3.96 kW; and at 6250 shaft speed, 5.89 kW of shaft work is achieved.

Fig. 7 (c) displays exhaust energy flows variation of JP5, JP5+HHO 1, JP5+HHO 1.5, JP5+HHO 2, and JP5+HHO 4 fuels at various shaft speeds. As shaft speed increases from 3250 to 6250 rpm, exhaust energy flows tend to increase. Minimum exhaust energy flows for all test fuels are observed at 3250 shaft speed, while maximum exhaust energy flows are achieved at 6250 shaft speed. For instance, at 3250 shaft speed, the exhaust energy flows for JP5, JP5+HHO 1, JP5+HHO 1.5, JP5+HHO 2, and JP5+HHO 4 fuels are 0.49 kW, 0.47 kW, 0.52 kW, 0.53 kW, and 0.49 kW respectively. At 6250 shaft speed, the exhaust energy flows for JP5, JP5+HHO 1, JP5+HHO 1.5, JP5+HHO 2, and JP5+HHO 4 fuels are 1.55 kW, 1.54 kW, 1.63 kW, 1.62 kW, and 1.47 kW respectively. According to Fig. 7 (c), it is evident that JP5+HHO 1.5 and JP5+HHO 2 fuels reach maximum values in exhaust energy flows between 3250 and

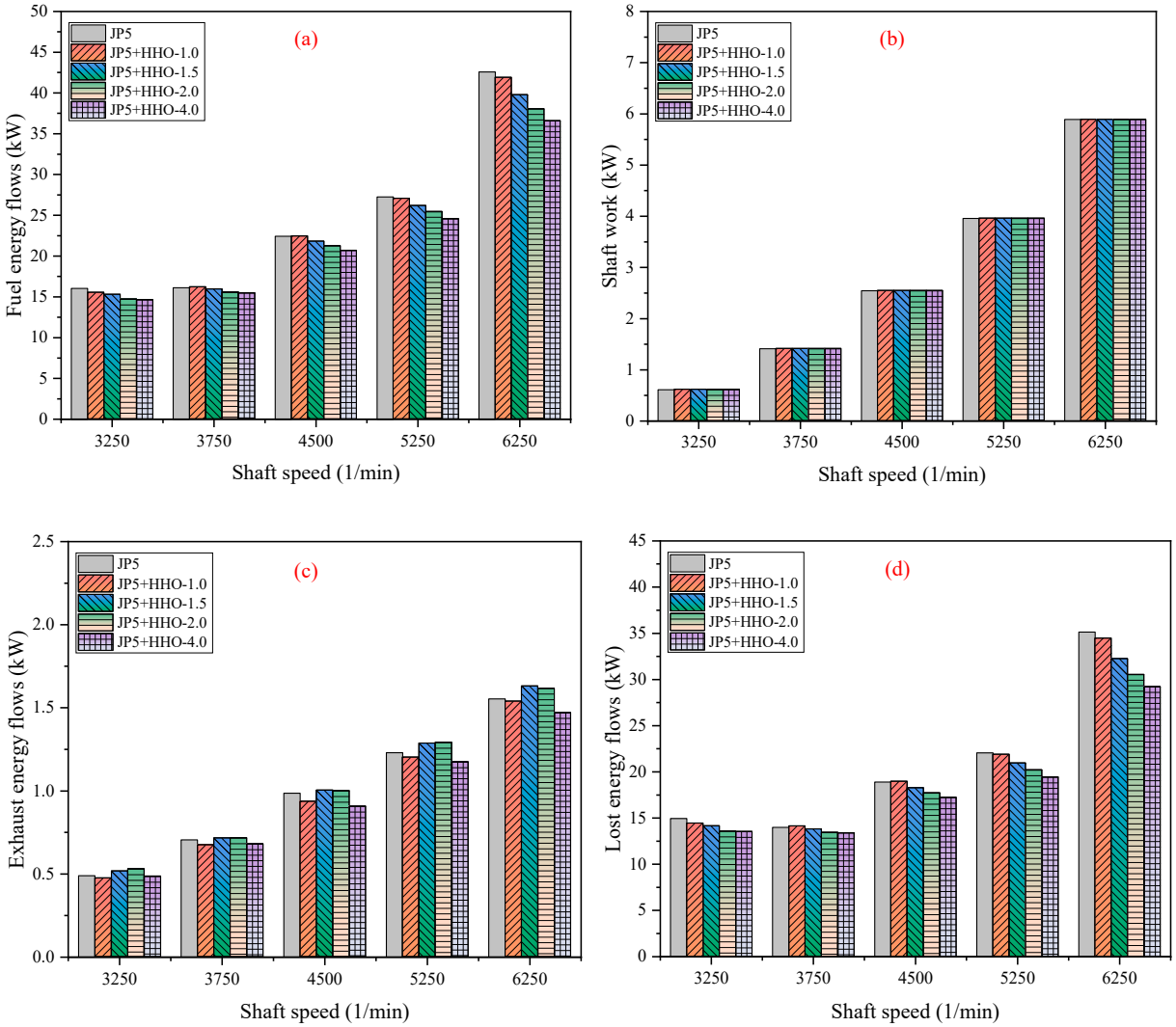

Fig. 7. (a)fuel energy flows, (b)shaft work, (c)exhaust energy flows, and (d)lost energy flows variation at different shaft speeds.

6250 shaft speeds, while JP5+HHO 1 and JP5+HHO 4 fuels have lower exhaust energy flows. This can be attributed to both the higher post-combustion products (such as CO2 gas) and the higher EGT values of JP5+HHO 1.5 and JP5+HHO 2 fuels compared to JP5+HHO 1 and JP5+HHO 4 fuels. Generally, in the 3250 to 6250 shaft speed range, compared to JP5 fuel, JP5+HHO 1 and JP5+HHO 4 fuels show average decreases of approximately 4% and 5% in exhaust energy flows respectively, while JP5+HHO 1.5 and JP5+HHO 2 fuels show average increases of approximately 4% and 4% respectively.

Fig. 7 (d) displays lost energy flows variation of JP5, JP5+HHO 1, JP5+HHO 1.5, JP5+HHO 2, and JP5+HHO 4 fuels at various shaft speeds. The system's maximum lost energy flows occur at 6250 shaft speed, while minimum loss energy flows occur at 3250 rpm. The primary reason for this is the significant increase in friction losses with increasing speed. Additionally, heat loss, lubricating oil loss, and many unaccounted parasitic losses tend to increase with speed. This phenomenon results in increased loss energy flows at higher speeds. Generally, the highest loss energy flows are observed with JP5 fuel, while the lowest loss energy flows are achieved in JP5+HHO dual fuel configurations. For example, at 3250 rpm shaft speed, the loss energy flows for JP5, JP5+HHO 1, JP5+HHO 1.5, JP5+HHO 2, and JP5+HHO 4 fuels are 14.9 kW, 14.4 kW, 14.2 kW, 13.6 kW, and 13.5 kW respectively. At 6250 rpm shaft speed, the loss energy flows for JP5, JP5+HHO 1, JP5+HHO 1.5, JP5+HHO 2, and JP5+HHO 4 fuels are 35.1 kW, 34.5 kW, 32.3 kW, 30.6 kW, and 29.2 kW respectively. In general, in the 3250–6250 rpm shaft speed range, compared to JP5 fuel, JP5+HHO 1, JP5+HHO 1.5, JP5+HHO 2, and JP5+HHO 4 fuels show average decreases in loss energy flows of approximately 1%, 5%, 8%, and 10% respectively.

Fig. 8 displays energy efficiency variation of JP5, JP5+HHO 1, JP5+HHO 1.5, JP5+HHO 2, and JP5+HHO 4 fuels at various shaft speeds. Both the increase in shaft speed from 3250 rpm upwards and the dual-fuel application of JP5 fuel with HHO contribute to improving energy efficiency. Minimum energy efficiency is achieved at 3250 rpm shaft speed, while maximum energy efficiency is achieved at 5250 rpm shaft speed. For example, at 3250 rpm shaft speed, the energy efficiency of JP5 fuel is 3.8%, whereas compared to JP5 fuel, JP5+HHO 1, JP5+HHO 1.5, JP5+HHO 2, and JP5+HHO 4 fuels show increases in energy efficiency of 3%, 5%, 9%, and 9% respectively. At 5250 rpm shaft speed, the energy efficiency of JP5 fuel is 14.5%, while JP5+HHO 1, JP5+HHO 1.5, JP5+HHO 2, and JP5+HHO 4 fuels show increases in energy efficiency of 1%, 4%, 7%, and 11% respectively compared to JP5 fuel. However, as shaft speed transitions from 5250 rpm to 6250 rpm, energy efficiency slightly decreases due to increased friction losses and other unaccounted losses. The dual-fuel application of JP5 fuel with HHO ensures high energy efficiency due to lower fuel consumption and reduced losses. Sharma et al. [27] reported that the addition of HHO to a diesel engine increases work availability. They attributed this to the high diffusivity of H_2, which improves the air/fuel mixture and enhances combustion. Overall, JP5+HHO 1, JP5+HHO 1.5, JP5+HHO 2, and JP5+HHO 4 fuels compared to JP5 fuel across the 3250–6250 rpm range, the average increases in energy efficiency are approximately 1%, 4%, 7%, and 10%, respectively.

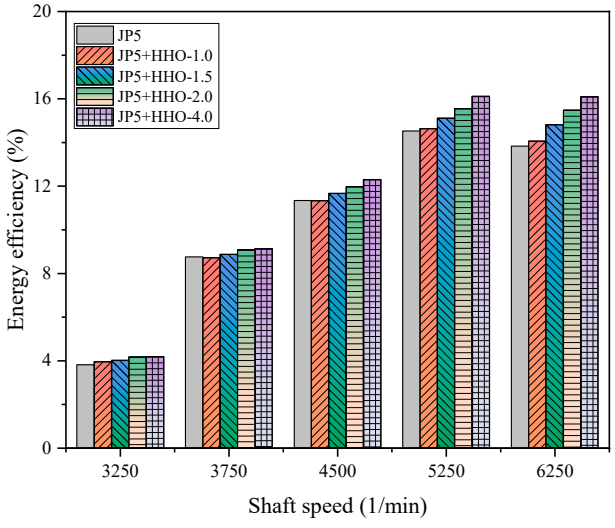

Fig. 8. Variation of energy efficiency of a two-stroke UAV engine at different shaft speeds.

3.3. Exergy analysis

Fig. 9 (a) displays fuel exergy flow variation of JP5, JP5+HHO 1, JP5+HHO 1.5, JP5+HHO 2, and JP5+HHO 4 fuels at various shaft speeds. In general, the JP5+HHO dual-fuel application contributes to a decrease in fuel exergy flows. This is due to the lower heating value of the dual fuel in conjunction with HHO usage, as well as lower mass fuel consumption. Minimum fuel exergy flows are achieved at 3250 rpm shaft speed, while maximum fuel exergy flows are achieved at 6250 rpm shaft speed. For example, at 3250 rpm shaft speed, the fuel exergy flows for JP5, JP5+HHO 1, JP5+HHO 1.5, JP5+HHO 2, and JP5+HHO 4 fuels are 17.2 kW, 16.6 kW, 16.3 kW, 15.7 kW, and 15.7 kW respectively. At 6250 rpm shaft speed, the fuel exergy flows for JP5, JP5+HHO 1, JP5+HHO 1.5, JP5+HHO 2, and JP5+HHO 4 fuels are 45.5 kW, 44.8 kW, 42.5 kW, 40.7 kW, and 39.1 kW respectively. At 3250 rpm shaft speed, the reduction rates in fuel exergy flows compared to JP5 fuel are 3.2%, 4.8%, 8.2%, and 8.7% for JP5+HHO 1, JP5+HHO 1.5, JP5+HHO 2, and JP5+HHO 4 fuels respectively. At 6250 rpm shaft speed, the reduction rates in fuel exergy flows compared to JP5 fuel are 1.6%, 6.6%, 10.6%, and 14% for JP5+HHO 1, JP5+HHO 1.5, JP5+HHO 2, and JP5+HHO 4 fuels respectively.

Fig. 9 (b) displays exhaust exergy flow variation of JP5, JP5+HHO 1, JP5+HHO 1.5, JP5+HHO 2, and JP5+HHO 4 fuels at various shaft speeds. Shaft speed increase correlates positively with exhaust exergy flows. This is because post-combustion products tend to increase with engine speed and power. Minimum exhaust exergy flows for all test fuels are observed at 3250 shaft speed, while maximum exhaust exergy flows are achieved at 6250 shaft speed. For instance, at 3250 shaft speed, the exhaust exergy flows for JP5, JP5+HHO 1, JP5+HHO 1.5, JP5+HHO 2, and JP5+HHO 4 fuels are 1.06 kW, 1 kW, 1.04 kW, 1.02 kW, and 1.02 kW respectively. At 6250 shaft speed, the exhaust exergy flows for JP5, JP5+HHO 1, JP5+HHO 1.5, JP5+HHO 2, and JP5+HHO 4 fuels are 2.57 kW, 2.41 kW, 2.47 kW, 2.38 kW, and 2.30 kW respectively. Between shaft speeds of 3250 rpm and 6250 rpm, JP5 fuel exhibits higher exhaust exergy flows compared to other fuels. This is likely due to higher mass airflow during single fuel usage, which increases the exhaust gas flow rate and consequently leads to notable increases in exhaust exergy flows. Literature includes studies demonstrating that the use of HHO can reduce the mass airflow. Also, the relatively similar EGT temperatures do not significantly influence the variation in exhaust exergy flows. In general, in the 3250–6250 rpm shaft speed range, compared to JP5 fuel, JP5+HHO 1, JP5+HHO 1.5, JP5+HHO 2, and JP5+HHO 4 fuels show average decreases in exhaust exergy flows of approximately 4%, 2%, 3%, and 5% respectively.

Fig. 9 (c) displays heat transfer exergy variation of JP5, JP5+HHO 1, JP5+HHO 1.5, JP5+HHO 2, and JP5+HHO 4 fuels at various shaft speeds. The minimum heat transfer exergy of the two-stroke air-cooled engine system is achieved at 3250 rpm shaft speed, while the maximum heat transfer exergy is obtained at 6250 rpm shaft speed. For instance, at 3250 rpm shaft speed, the heat transfer exergies of JP5, JP5+HHO 1, JP5+HHO 1.5, JP5+HHO 2, and JP5+HHO 4 fuels are 6.6 W, 6.8 W, 7.2 W, 7.4 W, and 7.0 W respectively. At 6250 rpm shaft speed, the heat transfer exergies for JP5, JP5+HHO 1, JP5+HHO 1.5, JP5+HHO 2, and JP5+HHO 4 fuels are 17.1 W, 17.9 W, 18.5 W, 19.1 W, and 18.5 W respectively. It is observed that the heat transfer exergy flows of

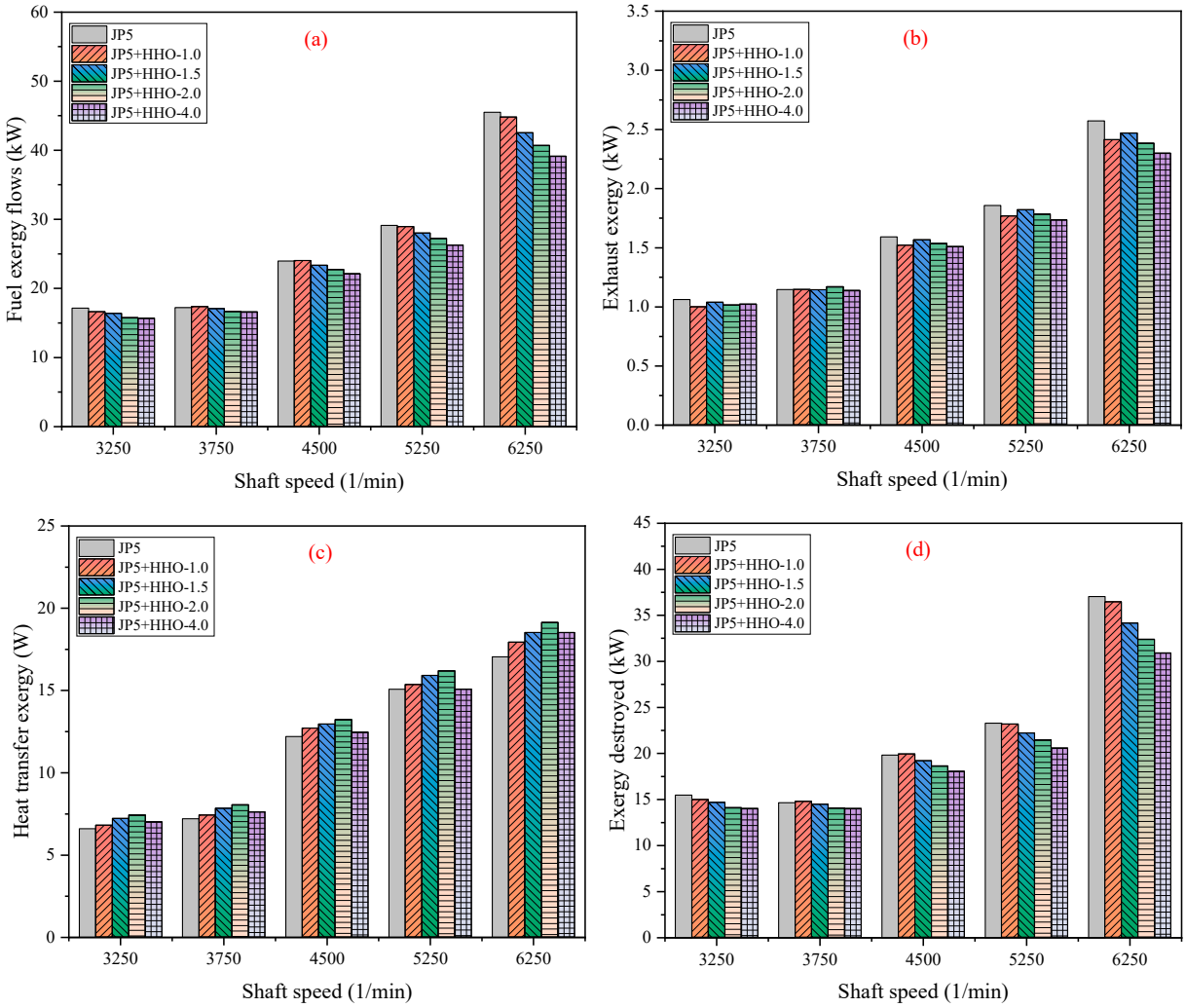

Fig. 9. (a)fuel exergy flows, (b)exhaust exergy flows, (c)heat transfer exergy, and (d)exergy destroyed variation at different shaft speeds.

JP5+HHO dual-fuel applications are higher compared to JP5 fuel alone. This is attributed to the increase in combustion gas temperatures due to H_2 in HHO, thereby increasing the heat transfer rate with ambient temperatures. Additionally, when examining the EST values in Fig. 5, the highest values are achieved with JP5+HHO dual-fuel application, whereas the lowest values are obtained with JP5 single-fuel application. This indicates why heat transfer rates are higher in HHO applications. Generally, the highest heat transfer exergy currents are achieved with JP5+HHO 2 fuel, followed by JP5+HHO 1.5 fuel. The H_2 in HHO possesses high flammability and adiabatic flame temperature. Therefore, when combustion occurs, the temperature of the burned gases rises significantly, increasing the heat transfer rate in air-cooled engines. However, an excessive increase in the amount of HHO in the cylinder raises the O_2 concentration and lowers the LHV of the mixture, leading to a decrease in combustion temperatures. As shown in Fig. 5, EST increases up to 2 L/min of HHO, but it decreases at 4 L/min of HHO gas. This is due to the excessive air/fuel ratio, resulting in weaker combustion conditions. Therefore, the highest heat transfer loss occurs with the JP5 + 2 L/min HHO dual-fuel application. Dhyani and Subramanian [70] also noted that increasing the H_2 concentration in the cylinder raises combustion temperatures, which in turn leads to higher heat transfer losses. In general, in the 3250–6250 rpm shaft speed range, compared to JP5 fuel, JP5+HHO 1, JP5+HHO 1.5, JP5+HHO 2, and JP5+HHO 4 fuels show average increases in heat transfer exergy flows of approximately 3%, 8%, 10%, and 5% respectively.

Fig. 9 (d) displays exergy destroyed variation of JP5, JP5+HHO 1, JP5+HHO 1.5, JP5+HHO 2, and JP5+HHO 4 fuels at various shaft speeds. JP5+HHO dual-fuel application is observed to have a significant impact on exergy destroyed compared to JP5 single-fuel application. Close minimum exergy destroyed values are obtained at 3250 rpm and 3750 rpm shaft speeds, whereas maximum exergy destruction occurs at 6250 rpm shaft speed. For instance, at 3250 rpm shaft speed, the exergy destroyed of JP5, JP5+HHO 1, JP5+HHO 1.5, JP5+HHO 2, and JP5+HHO 4 fuels are 15.5 kW, 15.0 kW, 14.7 kW, 14.1 kW, and 14.0 kW respectively. At 6250 rpm shaft speed, the exergy destroyed for JP5, JP5+HHO 1, JP5+HHO 1.5, JP5+HHO 2, and JP5+HHO 4 fuels are 37.0 kW, 36.5 kW, 34.2 kW, 32.4 kW, and 30.9 kW respectively. Generally, between 3250 rpm and 6250 rpm shaft speeds, JP5 and JP5+HHO 1 fuels exhibit the highest exergy destroyed, while an increasing ratio in HHO dual-fuel application tends to decrease exergy destroyed. The improvement of the combustion process by HHO is the main factor contributing to the reduction in exergy destroyed. On the other hand, lower fuel consumption and lower exhaust exergy flows to achieve the existing power also contribute to lower exergy destroyed levels. The increase in heat transfer exergy at higher HHO ratios, however, does not significantly affect exergy destroyed due to its very low amounts. In general, in the 3250–6250 rpm shaft speed range, compared to JP5 fuel, JP5+HHO 1, JP5+HHO 1.5, JP5+HHO 2, and JP5+HHO 4 fuels show average reductions in exergy destroyed of approximately 1%, 4%, 8%, and 10% respectively.

Fig. 10 displays irreversibilities variation of JP5, JP5+HHO 1, JP5+HHO 1.5, JP5+HHO 2, and JP5+HHO 4 fuels at various shaft

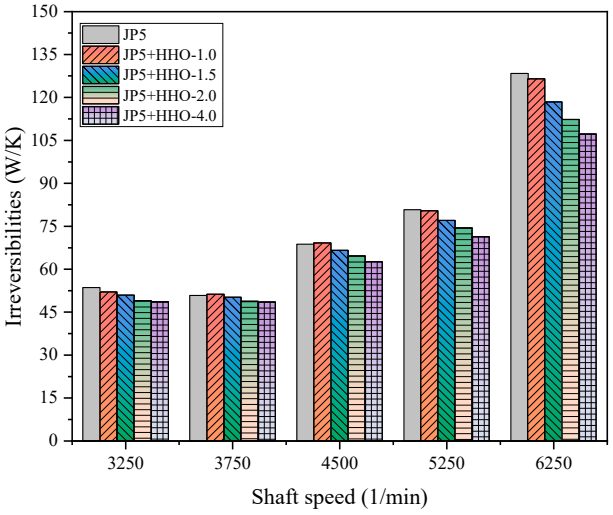

Fig. 10. Variation of irreversibilities of a two-stroke UAV engine at different shaft speeds.

speeds. The irreversibility of the two-stroke air-cooled engine are function of exergy destruction, and an increase in exergy destruction leads to increased irreversibilities. Fig. 10 shows that the use of HHO reduces engine irreversibilities, and this improvement becomes more significant at higher speeds. As engine speed increases, factors such as increased fuel injected into the cylinder and decreased volumetric efficiency contribute to increased irreversibilities. This results in longer combustion durations and increased combustion products, further increasing irreversibilities. At higher speeds, the use of JP5+HHO dual-fuel application increases H_2 and O_2 concentrations in the combustion zone, contributing to improved combustion processes and lower fuel consumption. Both reduced fuel consumption and improved combustion phase significantly contribute to reducing irreversibilities. At 3250 rpm shaft speed, the irreversibility value of JP5 fuel is 53.6 W/K, whereas JP5+HHO 1, JP5+HHO 1.5, JP5+HHO 2, and JP5+HHO 4 fuels show reductions in irreversibility values by 3%, 5%, 9%, and 9%, respectively. At the maximum irreversibilities observed at 6250 rpm shaft speed, JP5 fuel has an irreversibility of 128.4 W/K, while JP5+HHO 1, JP5+HHO 1.5, JP5+HHO 2, and JP5+HHO 4 fuels show reductions in irreversibility values by 2%, 8%, 13%, and 17%, respectively.

Fig. 11 displays exergy efficiency variation of JP5, JP5+HHO 1, JP5+HHO 1.5, JP5+HHO 2, and JP5+HHO 4 fuels at various shaft speeds. The two-stroke air-cooled UAV engine achieves its minimum exergy efficiency at 3250 rpm shaft speed, while maximum exergy efficiency is attained at 5250 rpm shaft speed. For instance, at 3250 rpm shaft speed, the exergy efficiencies of JP5, JP5+HHO 1, JP5+HHO 1.5, JP5+HHO 2, and JP5+HHO 4 fuels are 3.6%, 3.7%, 3.8%, 3.9%, and 3.9%, respectively. At 5250 rpm shaft speed, these efficiencies increase to 13.6%, 13.7%, 14.1%, 14.5%, and 15.1% for JP5, JP5+HHO 1, JP5+HHO 1.5, JP5+HHO 2, and JP5+HHO 4 fuels, respectively. The dual-fuel application of JP5+HHO significantly contributes to higher exergy efficiency due to lower fuel consumption and reduced exergy destroyed compared to JP5 single-fuel application. In his study using diesel, biodiesel, and HHO fuels, Forero [71] reported that the exergy efficiency of biodiesel decreased compared to diesel, but that the application of biodiesel + HHO with the use of HHO had a higher exergy efficiency. Ferero attributed this to the increase in the amount of HHO, which enhances the content of H_2 and O_2 in the combustion zone and improves combustion. This is consistent with the findings obtained in the current article. In general, in the 3250–6250 rpm shaft speed range, compared to JP5 fuel, JP5+HHO 1, JP5+HHO 1.5, JP5+HHO 2, and JP5+HHO 4 fuels show average increases in exergy efficiency of approximately 1%, 4%, 7%, and 10% respectively.

3.4. Exergoenviromental analysis

In this paper, analyses are carried out by taking into account CO_2 gases released after combustion and known as greenhouse gases as exergoenvironmental effects. Fig. 12 displays exergoenviromental impact variation of JP5, JP5+HHO 1, JP5+HHO 1.5, JP5+HHO 2, and JP5+HHO 4 fuels at various shaft speeds. Exergoenvironmental impact tends to increase as the shaft speed increases from 3250 to 6250 rpm. Minimum exergoenvironmental impact results are obtained at 3250 rpm shaft speed, while maximum exergoenvironmental impact results are obtained at 6250 rpm shaft speed. For example, running a two-stroke engine at 3250 rpm for one year results in exergoenvironmental impacts of 0.81 tons CO_2, 0.82 tons CO_2, 0.82 tons CO_2, 0.82 tons CO_2, and 0.79 tons CO_2 for JP5, JP5+HHO 1, JP5+HHO 1.5, JP5+HHO 2, and JP5+HHO 4 fuels, respectively. Additionally, running the same engine at 6250 rpm high speed for one year results in exergoenvironmental impacts of 7.67 tons CO_2, 7.75 tons CO_2, 7.78 tons CO_2, 7.89 tons CO_2, and 7.64 tons CO_2 for JP5, JP5+HHO 1, JP5+HHO 1.5, JP5+HHO 2, and JP5+HHO 4 fuels, respectively. Throughout all shaft speeds, the highest exergoenvironmental impact is achieved with JP5+HHO 2 fuel,

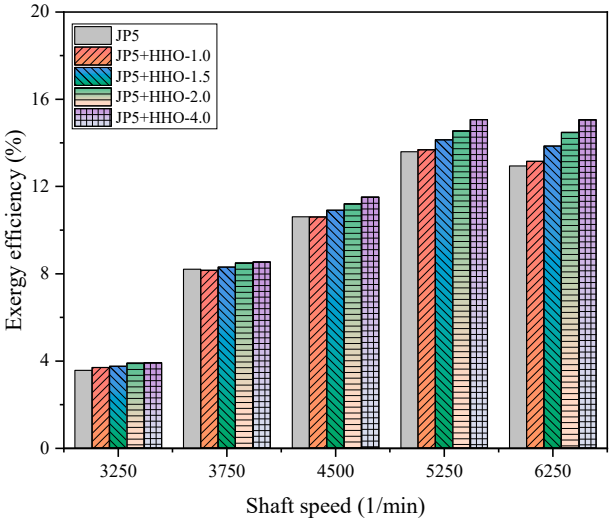

Fig. 11. Variation of exergy efficiency of a two-stroke UAV engine at different shaft speeds.

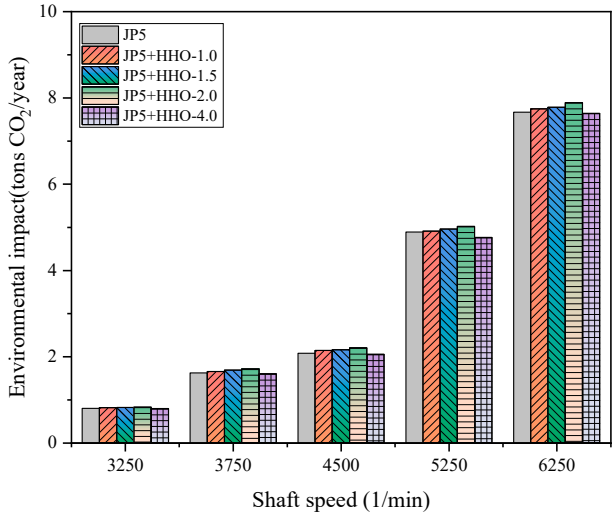

Fig. 12. Variation of exergoenviromental impact of a two-stroke UAV engine at different shaft speeds.

followed by JP5+HHO 1.5 fuel. This is because both fuels exhibit higher CO_2 emissions compared to other fuels. In general, in the 3250–6250 rpm shaft speed range, compared to JP5 fuel, JP5+HHO 1, JP5+HHO 1.5, and JP5+HHO 2 fuels show average increases in exergoenvironmental impact of approximately 1%, 2%, and 4% respectively. Conversely, the exergoenvironmental impact of JP5+HHO 4 fuel is reduced by approximately 2% on average compared to JP5 fuel.

3.4.1. Exergoenviroeconomic analysis

Fig. 13 displays exergoenviroeconomic impact variation of JP5, JP5+HHO 1, JP5+HHO 1.5, JP5+HHO 2, and JP5+HHO 4 fuels at various shaft speeds. When a two-stroke, air-cooled engine operates at 6250 rpm over the course of one year, the highest exergoenvironmental economic impact values are observed due to CO_2 emissions into the environment. For instance, running the engine at 6250 rpm for one year results in exergoenvironmental economic impacts of approximately €600/year, €606/year, €609/year, €617/year, and €597/year for JP5, JP5+HHO 1, JP5+HHO 1.5, JP5+HHO 2, and JP5+HHO 4 fuels, respectively. Conversely, operating the same engine at 3250 rpm for one year yields exergoenvironmental economic impacts of approximately €63/year, €64/year, €64/year, €64/year, and €62/year for JP5, JP5+HHO 1, JP5+HHO 1.5, JP5+HHO 2, and JP5+HHO 4 fuels, respectively. When the engine operates between 3250 rpm and 6250 rpm over the course of one year, the average exergoenvironmental economic impacts for JP5, JP5+HHO 1, JP5+HHO 1.5, JP5+HHO 2, and JP5+HHO 4 fuels are approximately €267/year, €270/year, €272/year, €276/year, and €264/year, respectively.

4. Conclusions

In this study, experiments of an engine with JP5 aviation fuel and HHO gas in dual-fuel mode at different shaft speeds were carried out. The energy, exergy, exergoenvironmental, and exergoeconomic evaluations based on these experimental data yield several important conclusions.

- **Fuel Efficiency:** The high diffusivity and enhanced oxygen content of HHO contribute to an average reduction in Brake Specific Fuel Consumption (BSFC) by 6%–11% compared to JP5. The use of 4 lpm of HHO leads to a 2% reduction in CO_2 emissions.
- **Exergy Efficiency and Reduction in Exergy Destruction:** HHO's positive impact on combustion improves fuel consumption and exergy efficiency. It also reduces exergy destruction, with a reduction ranging from 1% to 10% when increasing HHO from 1 to 4 lpm.
- **Heat Transfer Exergy:** Increasing HHO volume boosts combustion gas temperature, leading to a 3%–10% rise in heat transfer exergy.
- **Exergoenvironmental and Exergoeconomic Impacts:** While HHO increases energy and exergy efficiencies, it slightly elevates CO_2 emissions, leading to a 4% increase in exergoenvironmental and exergoeconomic impacts.

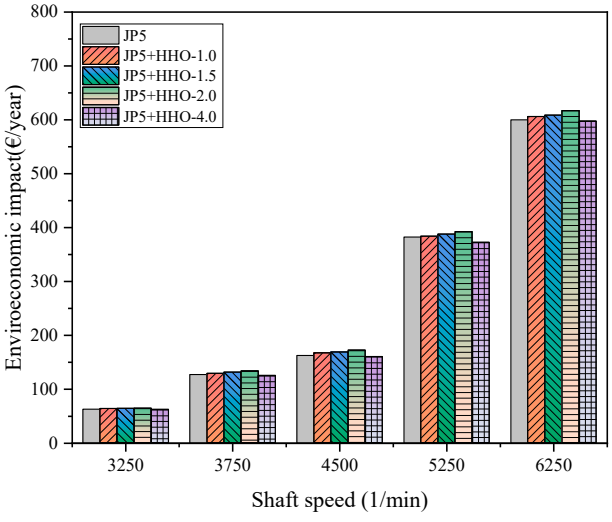

Fig. 13. Variation of exergoenviroeconomic impact of a two-stroke UAV engine at different shaft speeds.

4.1. Recommendations for industry and R&D

To further explore the potential of HHO as a sustainable fuel additive, the following recommendations are made.

1 Industry Application:
- **Optimization of HHO Integration:** Industries involved in UAV and small jet engines should consider optimizing HHO volume for fuel efficiency gains while monitoring environmental impacts. The current study shows that increasing HHO flow can reduce BSFC, but balancing this with emissions is crucial.
- **Development of HHO Injection Systems:** The development of advanced HHO injection systems to precisely control the flow rate (e.g., between 1 and 4 lpm) could allow for maximizing performance benefits while mitigating CO_2 emissions.
- **Pilot Studies in UAV Engines:** UAV manufacturers and defense industries should conduct pilot studies using the JP5+HHO blend to explore its viability in real-world conditions, especially for military and commercial UAV applications where energy efficiency is paramount.

2 Future R&D Directions:
- **HHO Enrichment with Hydrogen:** Future research should investigate enriching HHO with pure hydrogen to reduce carbon emissions, as indicated in this study. This could lower the exergoenvironmental impact, making it an even more sustainable option for the aviation industry.
- **Advanced Combustion Techniques:** Further research should focus on advanced combustion techniques (e.g., pre-chamber ignition systems) to enhance HHO combustion efficiency, thereby minimizing CO_2 emissions while boosting exergy efficiency.
- **Exploring Alternative Green Additives:** Beyond HHO, researchers should explore other green additives or dual-fuel blends (e.g., biofuels or ammonia) that can further enhance engine efficiency while reducing environmental impact.
- **Thermal Management Strategies:** Research into thermal management strategies could help better harness the increased heat transfer exergy caused by higher HHO volumes, potentially improving overall engine thermodynamic performance.

Generally, the use of HHO in dual fuel mode enhances energy and exergy efficiencies. However, it also leads to an increase in CO_2 emissions, which contributes to higher exergoenvironmental and exergoenviroeconomic impacts. In future studies, enriching HHO with H_2 could significantly reduce carbon emissions. This could lead to achieving lower environmental and economic impacts.

CRediT authorship contribution statement

S. Özer: Writing – original draft, Project administration, Methodology, Conceptualization. **E. Tunçer:** Supervision, Methodology, Investigation. **U. Demir:** Writing – original draft, Visualization, Investigation, Conceptualization. **H.E. Gülcan:** Writing – original draft, Visualization, Formal analysis, Conceptualization. **S. Çelebi:** Writing – original draft, Methodology, Data curation.

Declaration of interests

The authors declare that they have no known competing financial interests or personal relationships that could have appeared to influence the work reported in this paper.

References

[1] Mohsan SAH, Khan MA, Noor F, Ullah I, Alsharif MH. Towards the unmanned aerial Vehicles (UAVs): a comprehensive review. Drones 2022;6:147. https://doi.org/10.3390/DRONES6060147. 2022;6:147.

[2] Alotaibi A, Chatwin C, Birch P. Ubiquitous unmanned aerial Vehicles (UAVs): a comprehensive review. Shanlax Int J Arts, Sci Humanit 2023;11:62–90. https://doi.org/10.34293/SIJASH.V11I2.6650.

[3] Jaiswal S, Sidhanta S. Toward a smart multi-unmanned aerial vehicle system. IEEE Potentials 2022;41:22–5. https://doi.org/10.1109/MPOT.2021.3117259.

[4] Schneiderman R. Unmanned drones are flying high in the military/aerospace sector [Special Report]. IEEE Signal Process Mag 2012;29:8–11. https://doi.org/10.1109/MSP.2011.943127.

[5] Bhatt K, Pourmand A, Sikka N. Targeted applications of unmanned aerial Vehicles (drones) in telemedicine. Telemed J e Health 2018;24:833–8. https://doi.org/10.1089/TMJ.2017.0289.

[6] Mohammed AA, Shinkafi AA, Isah A, Ajayi JA, Pedro PT, Asooto BC, et al. Prospects and challenges of propulsion technologies of unmanned aerial Vehicles: a review. Niger J Technol 2021;40. https://doi.org/10.4314/NJT.V40I6.8. 1063-1071–1063 –1071.

[7] Velidi G, Yoo CS. A review on flame stabilization technologies for UAV engine micro-meso scale combustors: progress and challenges. Energies 2023;16:3968. https://doi.org/10.3390/EN16093968. 2023;16:3968.

[8] Wang Y, Shi Y, Cai M, Xu W, Zhang J, Zhong W, et al. Optimization of fuel injection control system of two-stroke aeroengine of UAV. Complexity 2020;2020:8921320. https://doi.org/10.1155/2020/8921320.

[9] Liu R, Sheng J, Ma J, Yang G, Dong X, Liang Y. Knock combustion investigation on a two-stroke spark ignition UAV engine burning RP-3 kerosene fuel. Aircr Eng Aerosp Technol 2019;91:1278–84. https://doi.org/10.1108/AEAT-08-2018-0232/FULL/PDF.

[10] Hassantabar A, Najjaran A, Farzaneh-Gord M. Investigating the effect of engine speed and flight altitude on the performance of throttle body injection (TBI) system of a two-stroke air-powered engine. Aerosp Sci Technol 2019;86:375–86. https://doi.org/10.1016/J.AST.2019.01.006.

[11] Cowart J, Foley MP, Luning Prak D. The development and testing of Navy jet fuel (JP-5) surrogates. Fuel 2019;249:80–8. https://doi.org/10.1016/J.FUEL.2019.03.096.

[12] Luning Prak DJ, Simms GR, Dickerson T, McDaniel A, Cowart JS. Formulation of 7-component surrogate mixtures for military jet fuel and testing in diesel engine. ACS Omega 2022;7:2275–85. https://doi.org/10.1021/ACSOMEGA.1C05904/ASSET/IMAGES/LARGE/AO1C05904_0007.JPEG.

[13] Lee H, Cameretti C. Spray, combustion, and air pollutant characteristics of JP-5 for naval aircraft from experimental single-cylinder CRDI diesel engine. Energies 2021;14:2362. https://doi.org/10.3390/EN14092362. 2021;14:2362.

[14] Bouguessa R, Tarabet L, Loubar K, Belmrabet T, Tazerout M. Experimental investigation on biogas enrichment with hydrogen for improving the combustion in diesel engine operating under dual fuel mode. Int J Hydrogen Energy 2020;45:9052–63. https://doi.org/10.1016/J.IJHYDENE.2020.01.003.

[15] eLibrary EPS. AUTO-IGNITION BEHAVIOR OF JP-5 SURROGATES IN A RAPID COMPRESSION MACHINE n.d. https://epslibrary.at/sgem_jresearch_publication_view.php?page=view&editid1=9065. [Accessed 22 July 2024].

[16] Baek HM, Lee HM. Spray behavior, combustion, and emission characteristics of jet propellant-5 and biodiesel fuels with multiple split injection strategies. Energies 2022;15:2540. https://doi.org/10.3390/EN15072540. 2022;15:2540.

[17] Lee H. Application of JP-5 in a CRDI diesel engine with various fuel injection distribution strategy. J Adv Mar Eng Technol 2021;45:243–51. https://doi.org/10.5916/JAMET.2021.45.5.243.

[18] Luning Prak D, Cowart J. Physical properties and diesel engine combustion of blends of alcohols with military jet fuel JP-5. Fuel 2024;371:132070. https://doi.org/10.1016/J.FUEL.2024.132070.

[19] Ning L, Duan Q, Wei Y, Zhang X, Yang B, Zeng K. Experimental investigation on combustion and emissions of a two-stroke DISI engine fueled with aviation kerosene at various compression ratios. Fuel 2020;259:116224. https://doi.org/10.1016/J.FUEL.2019.116224.

[20] Nabil T, Khairat Dawood MM. Enabling efficient use of oxy-hydrogen gas (HHO) in selected engineering applications; transportation and sustainable power generation. J Clean Prod 2019;237:117798. https://doi.org/10.1016/J.JCLEPRO.2019.117798.

[21] Al-Rousan AA. Reduction of fuel consumption in gasoline engines by introducing HHO gas into intake manifold. Int J Hydrogen Energy 2010;35:12930–5. https://doi.org/10.1016/J.IJHYDENE.2010.08.144.

[22] Salek F, Zamen M, Hosseini SV, Babaie M. Novel hybrid system of pulsed HHO generator/TEG waste heat recovery for CO reduction of a gasoline engine. Int J Hydrogen Energy 2020;45:23576–86. https://doi.org/10.1016/J.IJHYDENE.2020.06.075.

[23] Jakliński P, Czarnigowski J. An experimental investigation of the impact of added HHO gas on automotive emissions under idle conditions. Int J Hydrogen Energy 2020;45:13119–28. https://doi.org/10.1016/J.IJHYDENE.2020.02.225.

[24] Demir U, Çelebi S, Özer S. Experimental investigation of the effect of fuel oil, graphene and HHO gas addition to diesel fuel on engine performance and exhaust emissions in a diesel engine. Int J Hydrogen Energy 2024;52:1434–46. https://doi.org/10.1016/J.IJHYDENE.2023.08.007.

[25] Yilmaz AC, Uludamar E, Aydin K. Effect of hydroxy (HHO) gas addition on performance and exhaust emissions in compression ignition engines. Int J Hydrogen Energy 2010;35:11366–72. https://doi.org/10.1016/J.IJHYDENE.2010.07.040.

[26] Rimkus A, Matijošius J, Bogdevičius M, Bereczky Á, Török Á. An investigation of the efficiency of using O2 and H2 (hydrooxile gas -HHO) gas additives in a ci engine operating on diesel fuel and biodiesel. Energy 2018;152:640–51. https://doi.org/10.1016/J.ENERGY.2018.03.087.

[27] Kumar Sharma P, Sharma D, Lal Soni S, Jhalani A, Singh D, Sharma S. Energy, exergy, and emission analysis of a hydroxyl fueled compression ignition engine under dual fuel mode. Fuel 2020;265:116923. https://doi.org/10.1016/J.FUEL.2019.116923.

[28] Usman M, Malik MAI, Bashir R, Riaz F, Raza MJ, Suleman K, et al. Enviro-economic assessment of HHO–CNG mixture utilization in spark ignition engine for performance and environmental sustainability. Energies 2022;15:8253. https://doi.org/10.3390/EN15218253. 2022;15:8253.

[29] Krishna VM. Emissions control and performance evaluation of spark ignition engine with oxy-hydrogen blending. Int J Heat Technol 2018;36:118–24. https://doi.org/10.18280/IJHT.360116.

[30] Sun X, Liu H, Duan X, Guo H, Li Y, Qiao J, et al. Effect of hydrogen enrichment on the flame propagation, emissions formation and energy balance of the natural gas spark ignition engine. Fuel 2022;307:121843. https://doi.org/10.1016/J.FUEL.2021.121843.

[31] Haragopala Rao B, Shrivastava KN, Bhakta HN. Hydrogen for dual fuel engine operation. Int J Hydrogen Energy 1983;8:381–4. https://doi.org/10.1016/0360-3199(83)90054-X.

[32] Shivapuji AM, Dasappa S. Influence of fuel hydrogen fraction on syngas fueled SI engine: fuel thermo-physical property analysis and in-cylinder experimental investigations. Int J Hydrogen Energy 2015;40:10308–28. https://doi.org/10.1016/J.IJHYDENE.2015.06.062.

[33] Zhu H, Zhang Y, Liu F, Wei W. Effect of excess hydrogen on hydrogen fueled internal combustion engine under full load. Int J Hydrogen Energy 2020;45:20419–25. https://doi.org/10.1016/J.IJHYDENE.2019.12.022.

[34] Gad MS, El-Fakharany MK, Elsharkawy EA. Effect of HHO gas enrichment on performance and emissions of a diesel engine fueled by biodiesel blend with kerosene additive. Fuel 2020;280:118632. https://doi.org/10.1016/J.FUEL.2020.118632.

[35] Aydin K, Kenanoğlu R. Effects of hydrogenation of fossil fuels with hydrogen and hydroxy gas on performance and emissions of internal combustion engines. Int J Hydrogen Energy 2018;43:14047–58. https://doi.org/10.1016/J.IJHYDENE.2018.04.026.

[36] Musmar SA, Al-Rousan AA. Effect of HHO gas on combustion emissions in gasoline engines. Fuel 2011;90:3066–70. https://doi.org/10.1016/J.FUEL.2011.05.013.

[37] Subramanian B, Thangavel V. Analysis of onsite HHO gas generation system. Int J Hydrogen Energy 2020;45:14218–31. https://doi.org/10.1016/J.IJHYDENE.2020.03.159.

[38] Polverino P, D'Aniello F, Arsie I, Pianese C. Study of the energetic needs for the on-board production of Oxy-Hydrogen as fuel additive in internal combustion engines. Energy Convers Manag 2019;179:114–31. https://doi.org/10.1016/J.ENCONMAN.2018.09.082.

[39] Chintala V, Subramanian KA. CFD analysis on effect of localized in-cylinder temperature on nitric oxide (NO) emission in a compression ignition engine under hydrogen-diesel dual-fuel mode. Energy 2016;116:470–88. https://doi.org/10.1016/J.ENERGY.2016.09.133.

[40] Zhang B, Wang H, Wang S. Computational investigation of combustion, performance, and emissions of a diesel-hydrogen dual-fuel engine. Sustain Times 2023;15. https://doi.org/10.3390/SU15043610. 3610 2023;15:3610.

[41] Kakoee A, Bakhshan Y, Aval SM, Gharehghani A. An improvement of a lean burning condition of natural gas/diesel RCCI engine with a pre-chamber by using hydrogen. Energy Convers Manag 2018;166:489–99. https://doi.org/10.1016/J.ENCONMAN.2018.04.063.

[42] Kenanoğlu R, Baltacıoğlu MK, Demir MH, Erkınay Özdemir M. Performance & emission analysis of HHO enriched dual-fuelled diesel engine with artificial neural network prediction approaches. Int J Hydrogen Energy 2020;45:26357–69. https://doi.org/10.1016/J.IJHYDENE.2020.02.108.

[43] Şöhret Y, Kıncay O, Karakoç TH. Combustion efficiency analysis and key emission parameters of a turboprop engine at various loads. J Energy Inst 2015;88(4):490–9. https://doi.org/10.1016/j.joei.2014.09.010.

[44] Badami M, Nuccio P, Pastrone D, Signoretto A. Performance of a small-scale turbojet engine fed with traditional and alternative fuels. Energy Convers Manag 2014;82:219–28. https://doi.org/10.1016/j.enconman.2014.03.026.

[45] Karpiński P, Pietrykowski K, Grabowski Ł. Turbocharging the aircraft two-stroke diesel engine. Combustion Engines 2019;58. https://doi.org/10.19206/CE-2019-319.

[46] Sundararaj RH, Kumar RD, Raut AK, Sekar TC, Pandey V, Kushari A, Puri SK. Combustion and emission characteristics from biojet fuel blends in a gas turbine combustor. Energy 2019;182:689–705. https://doi.org/10.1016/j.energy.2019.06.060.

[47] Korres DM, Karonis D, Lois E, Linck MB, Gupta AK. Aviation fuel JP-5 and biodiesel on a diesel engine. Fuel 2008;87:70–8. https://doi.org/10.1016/J.FUEL.2007.04.004.

[48] Gülcan HE. Effect of intake valve lift and binary alcohol (bioethanol+isobutanol) addition on energy, exergy, sustainability, greenhouse gas impact and cost analysis in a hydrogen/diesel dual fuel engines. Int J Hydrogen Energy 2024;77:450–71. https://doi.org/10.1016/J.IJHYDENE.2024.06.151.
[49] Canakci M, Hosoz M. Energy and exergy analyses of a diesel engine fuelled with various biodiesels. Energy Sources, Part B 2006;1:379–94. https://doi.org/10.1080/15567240500400796.
[50] Hoseinpour M, Sadrnia H, Tabasizadeh M, Ghobadian B. Energy and exergy analyses of a diesel engine fueled with diesel, biodiesel-diesel blend and gasoline fumigation. Energy 2017;141:2408–20. https://doi.org/10.1016/J.ENERGY.2017.11.131.
[51] Gülcan HE. Effect of methane injection strategy on combustion, exergetic performance, and enviro-economic analyses in a diesel/methane CRDI engine. Appl Therm Eng 2024;243:122654. https://doi.org/10.1016/J.APPLTHERMALENG.2024.122654.
[52] Nabi MN, Rasul MG, Anwar M, Mullins BJ. Energy, exergy, performance, emission and combustion characteristics of diesel engine using new series of non-edible biodiesels. Renew Energy 2019;140:647–57. https://doi.org/10.1016/J.RENENE.2019.03.066.
[53] Karthickeyan V, Thiyagarajan S, Ashok B, Edwin Geo V, Azad AK. Experimental investigation of pomegranate oil methyl ester in ceramic coated engine at different operating condition in direct injection diesel engine with energy and exergy analysis. Energy Convers Manag 2020;205:112334. https://doi.org/10.1016/J.ENCONMAN.2019.112334.
[54] Chaudhary V, Gakkhar R. Exergy based performance comparison of DI diesel engine fuelled with WCO15 and NEEM15 biodiesel. Environ Prog Sustain Energy 2020;39:e13363. https://doi.org/10.1002/EP.13363.
[55] Kotas TJ. Exergy method of thermal and chemical plant analysis. Chem Eng Res Des 1986;64:3.
[56] Rufino CH, de Lima AJTB, Mattos AP, Bernal JLL, Ferreira JV, et al. Exergetic analysis of a spark ignition engine fuelled with ethanol. Energy Convers Manag 2019;192:20–9. https://doi.org/10.1016/J.ENCONMAN.2019.04.035.
[57] Moran MJ, Shapiro HN, Boettner DD, Bailey MB (Margaret B. Fundamentals of engineering thermodynamics n.d.:1042.
[58] Caliskan H, Tat ME, Hepbasli A. Performance assessment of an internal combustion engine at varying dead (reference) state temperatures. Appl Therm Eng 2009;29:3431–6. https://doi.org/10.1016/J.APPLTHERMALENG.2009.05.021.
[59] Örs İ, Yelbey S, Gülcan HE, Sayın Kul B, Ciniviz M. Evaluation of detailed combustion, energy and exergy analysis on ethanol-gasoline and methanol-gasoline blends of a spark ignition engine. Fuel 2023;354:129340. https://doi.org/10.1016/J.FUEL.2023.129340.
[60] Karagoz M, Uysal C, Agbulut U, Saridemir S. Exergetic and exergoeconomic analyses of a CI engine fueled with diesel-biodiesel blends containing various metal-oxide nanoparticles. Energy 2021;214:118830. https://doi.org/10.1016/J.ENERGY.2020.118830.
[61] Yesilyurt MK, Arslan M. Analysis of the fuel injection pressure effects on energy and exergy efficiencies of a diesel engine operating with biodiesel. Biofuels 2019;10:643–55. https://doi.org/10.1080/17597269.2018.1489674.
[62] Demirbas M, Yesilyurt MK. Investigation of the behaviors of higher alcohols in a spark-ignition engine as an oxygenated fuel additive in energy, exergy, economic, and environmental terms. J Therm Anal Calorim 2023;148:4427–62. https://doi.org/10.1007/S10973-023-11993-W/TABLES/8.
[63] Demirbas M, Yesilyurt MK. Investigation of the behaviors of higher alcohols in a spark-ignition engine as an oxygenated fuel additive in energy, exergy, economic, and environmental terms. J Therm Anal Calorim 2023;148:4427–62. https://doi.org/10.1007/S10973-023-11993-W/METRICS.
[64] Yildiz I, Açıkkalp E, Caliskan H, Mori K. Environmental pollution cost analyses of biodiesel and diesel fuels for a diesel engine. J Environ Manage 2019;243:218–26. https://doi.org/10.1016/J.JENVMAN.2019.05.002.
[65] EU Carbon Permits - Price - Chart - Historical Data - News n.d. https://tradingeconomics.com/commodity/carbon (accessed March 16, 2024).
[66] Wei L, Geng P. A review on natural gas/diesel dual fuel combustion, emissions and performance. Fuel Process Technol 2016;142:264–78. https://doi.org/10.1016/J.FUPROC.2015.09.018.
[67] Heywood JB. Internal combustion engine fundamentals. 1988. p. 930.
[68] Pulkrabek WW. Engineering fundamentals of the internal combustion engine 2004:478.
[69] Kamarudin R, Ang YZ, Topare NS, Ismail MN, Mustafa KF, Gunnasegaran P, et al. Influence of oxyhydrogen gas retrofit into two-stroke engine on emissions and exhaust gas temperature variations. Heliyon 2024;10:e26597. https://doi.org/10.1016/J.HELIYON.2024.E26597/ASSET/F78FCD5D-026A-472C-80ED-7EEB38B2FB5A/MAIN.ASSETS/GR26.JPG.
[70] Dhyani V, Subramanian KA. Experimental based comparative exergy analysis of a multi-cylinder spark ignition engine fuelled with different gaseous (CNG, HCNG, and hydrogen) fuels. Int J Hydrogen Energy 2019;44:20440–51. https://doi.org/10.1016/J.IJHYDENE.2019.05.229.
[71] Forero JD. Energy, exergy and environmental assessment of partial fuel substitution with hydroxy powered by a thermoelectric generator in low displacement diesel engines. Clean Eng Technol 2021;3:100086. https://doi.org/10.1016/J.CLET.2021.100086.